IOS

DEACON LABORATORY

SURVEY OF INSTRUMENTAL METHODS FOR THE DETERMINATION OF THE HIGH FREQUENCY WAVE SPECTRUM

BY
C.H. CLAYSON

REPORT NO. 267
1989

Natural Environment Research Council

INSTITUTE OF OCEANOGRAPHIC SCIENCES
DEACON LABORATORY

INSTITUTE OF OCEANOGRAPHIC SCIENCES

DEACON LABORATORY

Wormley, Godalming,
Surrey, GU8 5UB, U.K.

Telephone: 0428 79 4141
Telex: 858833 OCEANS G
Telefax: 0428 79 3066

Director: Dr. C.P. Summerhayes

Natural Environment Research Council

INSTITUTE OF OCEANOGRAPHIC SCIENCES

DEACON LABORATORY

REPORT NO. 267

Survey of instrumental methods for the determination of the high frequency wave spectrum

C.H. Clayson

1989

DOCUMENT DATA SHEET

AUTHOR
CLAYSON, C.H.

PUBLICATION DATE 1989

TITLE
Survey of instrumentation methods for the determination of the high frequency wave spectrum.

REFERENCE
Institute of Oceanographic Sciences Deacon Laboratory, Report, No.267, 68pp.

ABSTRACT

Interest in the high frequency wave spectrum has increased because of the importance of decimetric and centimetric wavelength sea surface waves in microwave scattering processes.

This survey examines existing contact (surface-piercing) and non-contact (remote) sensing techniques for observing high frequency waves both in the time domain and spatially. It considers the defects and limitations of such techniques and how these might be overcome by alternative, largely untried, techniques.

Whilst apparently adequate instruments exist for time domain measurements in laboratory tanks, reservoirs, or small lakes, the observed nature of high frequency waves suggests that an adequate description of the processes can only be achieved by spatial measurements using, for example, high resolution stereophotography, in the open sea.

ISSUING ORGANISATION
Institute of Oceanographic Sciences
Deacon Laboratory
Wormley, Godalming
Surrey GU8 5UB. UK.

TELEPHONE 0428 79 4141
TELEX 858833 OCEANS G
TELEFAX 0428 79 3066

KEYWORDS
CAPILLARY WAVES
HIGH FREQUENCY
REMOTE SENSING
WAVE MEASURING EQUIPMENT
WAVE SPECTRA
WAVE STAFF SENSORS

CONTRACT

PROJECT

PRICE
£19.00

CONTENTS

1. PROJECT OBJECTIVES

To assess the feasibility of techniques which might be used to determine the characteristics of sea waves within the wavelength range applicable to backscattering of energy in remote microwave sensing. These objectives were to be met by:

(a) a comprehensive review of the literature in order to identify any techniques potentially suited to the measurement of wave motions at centimetric wavelengths,

(b) consideration of any new techniques which might be pursued for the purpose.

2. BACKGROUND

Interest in the high frequency end of the wave spectrum stems mainly from current developments in the field of remote sensing of the sea surface by active microwave techniques; there is also a general scientific interest on account of the (incompletely-understood) role of such waves in energy transfer processes at the air-sea interface. These processes include wind-wave generation, nonlinear energy transfer from short waves to long waves, dissipation of energy and wave breaking/spilling processes; see, for example, PHILLIPS (1977).

The particular importance of high frequency water waves in microwave remote sensing lies in Bragg scattering. Microwave energy incident upon the water surface may be specularly reflected, by facets which have structural detail of length scale much greater than the microwave wavelength; it is also scattered, by structure of length scale comparable to, or less than, the microwave wavelength. The energy returned to the remote sensing receiver from the sea is normally described by radar engineers (SKOLNIK, 1970) in terms of the "clutter coefficient" or radar cross section per unit area illuminated (normalised radar cross section NRCS), σ°. Over the past 15 years, or so, a great deal of attention has been focussed upon the variation of σ° with sea state and wind speed, as is evident from the considerable number of publications on the subject.

A knowledge of the dependence of microwave returns upon the various wave components is important, primarily in the interpretation of methods for the remote sensing of waves and winds by measurement of backscattered microwave radiation, but also in precise radar altimetry. Variations of backscattering over the gravity wave profiles can significantly bias the estimates of mean water level. Significant wave height as derived from altimeter return pulse shape is also affected by similar considerations.

Specular reflecting surfaces (facets) normal to the radar beam, and thus producing returns, will be transitory in nature and, due to the restricted range of slopes at the sea surface (0 to 30° from the horizontal in non-breaking waves) will only contribute to microwave returns for relatively near-nadir beam angles (in the case of monostatic radars). SCHOOLEY (1962) gives probability distributions for such facets. VALENZUELA (1978) gives a comprehensive summary of work on this subject.

The major contribution to returns at large angles from nadir results from Bragg resonant scattering, where constructive interference takes place for microwave wavelets scattered from sea surface structure which is periodic in the direction of the radar beam and has a wavelength (when resolved in the direction of the microwave beam axis) of $n\lambda_m/2$, where n is an integer (the order of the scattering process) and λ_m is the microwave wavelength (Figure 1).

The water wavelength, λ_w, which results in coherent scattering, is thus given by:

$$\lambda_w = 0.5\ n.\lambda_m\ \text{cosec}\ (\theta_1 - \theta_c)$$

where θ_1 is the angle of incidence (between the beam axis and nadir) and $\tan\theta_c$ is the local slope of the longer gravity "carrier" wave upon which the high frequency wave involved in Bragg scattering process rides.

The range of water wavelengths, λ_w, involved in first order Bragg scattering of radiation in typical satellite-borne radars, scatterometers, etc., can be calculated from published instrumental specifications to be approximately 30 cm to 1cm. This corresponds to a wave frequency range of 2.3Hz to 24.6Hz. These waves are in the gravity-capillary range where both gravity and surface tension are significant restoring forces in the oscillatory wave motion. There is some evidence that, at higher microwave frequencies, second order scattering is more important than first order (FISCELLA et al. 1985). Such gravity-capillary waves are present in most conditions, excepting flat calms and where there is surface contamination by oil slicks. The latter were amongst the first sea surface features to be identified in microwave imagery of the sea surface, due to their low $\sigma°$.

KWOH and LAKE (1984) have adopted a different approach to the generally accepted Bragg scattering explanation of non-specular returns by explaining scattering from the region of the sharp crests of the longer limiting amplitude waves in terms of scattering from wedges, using Keller's Geometric Theory of Diffraction (KELLER, 1962), rather than in terms of Bragg scattering.

The visibility of long gravity waves in synthetic aperture radar (SAR) imagery is due to variations of $\sigma°$ over the long wave profiles. This is held to be principally due to two mechanisms. The first of these is the modulation of the wavelength (and hence spectral density) of the gravity-capillary waves

that are involved in Bragg scattering by the slopes θ_c of the longer gravity "carrier" waves; this is usually referred to as "tilt modulation". The second is due to windspeed-dependent spatial modulation of the surface roughness due to "straining" by the horizontal velocities of the longer "carrier" gravity waves; this is usually referred to as "hydrodynamic modulation".

DURDEN and VESECKY (1985) have proposed a model for σ° in terms of quasi-specular scattering, Bragg scattering and the directional wave spectrum, with supporting experimental results. JONES and SCHROEDER (1978) considered the dependence of σ° upon the surface friction velocity over a microwave frequency range of 0.4 to 13.9 GHz.

SCHROEDER et al. (1985) give results obtained with a 13.9 GHz scatterometer, flown in an aircraft, over a range of wind speeds, v, and with various angles of incidence from nadir, θ, in the range 0 to 60°. Their results can be summarised as follows:

(a) for θ less than 20°, σ° is more or less independent of polarisation; over this range of θ, returns are largely due to specular reflection and the ratio of the reflection coefficients R_h/R_v for horizontal and vertical polarisation varies from 1.00 to 1.21 (Figure 2).

(b) For θ greater than 20°, σ° is more affected by θ and v in the case of horizontal polarisation, presumably since R_h is small close to the Brewster angle of 53°.

(c) For θ less than about 12°, σ° decreases with increasing wind speed, presumably due to reduction in specularly reflecting facet area.

(d) In the range $12^\circ<\theta<30^\circ$, $d\sigma^\circ/dv$ becomes increasingly positive. This is presumably due to increasing dependence upon Bragg scattering. For θ greater than 30°, $d\sigma^\circ/dv$ is more or less constant.

(e) For $\theta \sim 60^\circ$, σ° looking upwind is about double the downwind value (indicating that there are more scatterers on downwind slopes of the waves). Whilst $d\sigma^\circ/dv$ and $d\sigma^\circ/d\theta$ are similar in both up- and down-wind directions, $d\sigma^\circ/dv$ is significantly greater in the cross-wind direction. .This may indicate some windspeed-dependent directionality in the high frequency waves.

(f) At high wind speeds, σ° is much more dependent upon θ than upon polarisation or direction relative to the wind.

As mentioned previously, there is now a considerable wealth of published literature on the relation between microwave backscatter and wave/wind conditions. It has only been possible to mention a few examples here.

2(a) The high frequency wave spectrum

A general expression for the "deep-water" approximation for the relation between the wave phase velocity, C, and wavelength, λ, is given by:

$$C^2 = \frac{g.\lambda}{2\pi} + \frac{2\pi S}{\rho.\lambda}$$

$$= \frac{g}{k} + \frac{k.S}{\rho}$$

where g = gravitational acceleration (9.81 ms^{-2})
S = surface tension (~7.4 10^{-2} Nm^{-1})
ρ = density of water (~1 to 1.03 10^3 $kg.m^{-3}$)
k = wave number (= $2\pi/\lambda$ m^{-1})

The terms due to gravity and to surface tension are, thus, quite separate. The resulting wave frequency, f, is given by:

$$f = C/\lambda$$

$$f^2 = \frac{g}{2\pi\lambda} + \frac{2\pi S}{\lambda^3 \rho}$$

The relation between phase velocity, frequency and wavelength is shown in figure 3. The minimum phase velocity occurs at a wavelength λ_m, given by:

$$\lambda_m^2 = 4\pi^2 \frac{S}{g.\rho}$$

This wavelength is approximately 1.7 cm, corresponding to a frequency of approximately 13.5 Hz, and being slightly dependent upon salinity and temperature.

In taking measurements of these high frequency waves, the situation is complicated to some extent by the observed nature of the spatial distribution of such waves. Since they are quite rapidly attenuated, they are relatively transient phenomena which are more apparent in the regions of their

generation, whether by wind or by instabilities or discontinuities in the carrier waves, such as sharp crests, or breaking events. On sharp-crested gravity waves, saturated higher frequency gravity-capillary waves, arising from the slope discontinuity at the crest, are normally observed on the advancing side of the wave crest; less prominent, lower frequency, gravity-capillary waves are found on the back face of the crest. The generation of these gravity-capillary waves has been discussed by LONGUET-HIGGINS (1963) and further developed by CRAPPER (1970).

Since they are carried on gravity waves with considerable horizontal velocity components, Eulerian observations of the high frequency waves show modulation in apparent frequency; this has recently been demonstrated in measurements on a lake by ATAKTURK and KATSAROS (1987). It is unfortunate that the wavelength for minimum phase velocity (and hence maximimum Doppler shift by longer gravity wave velocities) lies in the range responsible for the first order Bragg scattering of X-band radiation. As a result of the above factors, representation in terms of a frequency spectrum may not be as useful as a wavenumber spectrum in studies of microwave scattering. Due to considerations of the advection and inertial processes involved at these high wave frequencies, it is not possible to use the simple dispersion relationship to convert from one form of the spectrum to the other. Despite this, it is worth remarking that most direct high frequency wave measurements and measuring techniques are, of necessity, based upon time series of elevation or slope at a point; the following review will not be limited to either of these approaches.

Notwithstanding the above remark regarding the use of the frequency spectrum to adequately describe the high frequency end of the wave spectrum, various workers have derived forms for the frequency spectrum E(f), both theoretically and empirically. The main interest originally lay in the most energetic part of the gravity wave spectrum. Later, when interest in high frequency waves arose, spectral forms were proposed for a number of ranges in the overall wave spectrum. These ranges were classified by PIERSON and STACY (1973) as the Pierson-Moskowitz range (the energetic gravity wave range of the spectrum), the Kitaigorodskii range (the high frequency end of the gravity wave region), the Leykin-Rosenberg range (the gravity-capillary wave region where restoring forces due to gravity and surface tension are both significant), the capillary range, and the Cox viscous cutoff range. This report is primarily concerned with the three intermediate ranges.

PHILLIPS (1958) proposed a theoretical form for E(f) for the upper end of the gravity wave range, which he considered to be an "equilibrium range" limited by wave breaking. On dimensional grounds, he proposed a spectrum of the form:

$$E(f) = \alpha . g^2 f^{-5}$$

where α is a dimensionless "equilibrium constant" and g is the gravitational acceleration. The above equilibrium range is defined by $f_o << f << f_m$, where f_o is the lowest frequency for which non-linear effects are important and f_m is the frequency for minimum phase velocity, as defined above.

This representation was subsequently questioned by a number of workers in the field who produced evidence of wind speed dependence of the energy levels. In particular, HASSELMANN et al. (1973) showed that α is, in fact, dependent upon the dimensionless fetch $Fg/(u_*)^2$, where F is the fetch and u_* is the friction velocity. There have been many published results confirming the f^{-5} law, to a greater or lesser degree of certainty.

The corresponding instantaneous spatial (wave number) spectrum, for a surface having simple discontinuities in slope, was given by PHILLIPS (1958) as:

$$\psi(k) = f(\theta).k^{-4}$$

where $f(\theta)$ is the directional distribution. This leads to a one dimensional (single direction) spectrum of the form:

$$\psi_1(k) = \beta k^{-3}$$

Phillips subsequently revised his proposed spectral forms (PHILLIPS,1985). His revised theory resulted in spectra of the form:

$$E(f) = \alpha g u_* f^{-4}$$

for the tail of the spectrum up to frequencies where Doppler shifting is significant

and $\psi_1(k) = B u_* g^{-1/2} k^{-5/2}$.

Phillips also suggests that there is a high frequency cut-off, due to suppression of freely travelling gravity waves of phase speed less than the surface drift velocity (= u_* in the down-wind direction). This could result in a "spectral gap" between gravity waves having a wavenumber of g/u_*^2 and the capillary wave spectrum. At higher wind speeds, this gap could be appreciable; qualitative visual observations possibly support its existence. The wavelength range affected is of importance to microwave backscatter.

DOBSON (1970) has achieved results, using stereophotographic techniques, which confirm the k^{-3} law. He reported that there was no apparent directionality at the frequencies observed ($k>3.3\ m^{-1}$) over a range of about ±45° relative to the wind direction. PIERSON and STACY (1973) suggested that β should be replaced by a wind speed dependent term $D(u_*)$. PIERSON (1976) subsequently proposed a spectrum, based on the data of MITSUYASU and HONDA (1974), of the form:

$$E(f) = 0.1393\ f^{-n}$$

where $n = 5 - \log_{10}u_*$, for the range 10 to 30 Hz.

KITAIGORODSKII (1961) derived the spectrum for the gravity-capillary range, on a different dynamical basis, as:

$$E(f) \sim Gu_*gf^{-4}$$

whilst TOBA (1973) gives a more refined form, with dependence of the wind speed term upon wave number, as:

$$E(f) = (2\pi)^{-3}\ \alpha_g u_* g_* f^{-4}$$

where α_g is a constant (~0.02), u_* is the friction velocity and $g_* = g + \gamma k^2$, where γ is the ratio of the surface tension to the density, and k is the wave number.

The Toba form, which gives an $f^{-8/3}$ law in the region of the spectrum dominated by surface tension, was supported by experimental work by MITSUYASU and HONDA (1974), who carried out measurements in a wind-wave channel, and again by MITSUYASU (1977) in measurements from a tower in the open sea.

KITAIGORODSKII (1973) gives the spectrum for the range $f_m<<f<<f_v$, where f_m is the frequency for minimum phase velocity and f_v is the frequency at which viscous damping becomes important (ca. 10^3 Hz), as:

$$E(f) = \beta\gamma^{2/3}f^{-7/3}$$

The $f^{-7/3}$ law has received support from LIU and LIN (1982) based upon wind-wave tank measurements, using an optical sensing system, for frequencies above 10 Hz.

KONDO, FUJINAWA and NAITO (1973) obtained a spectrum with approximately f^{-4} dependence over the range 1.5 to 10 Hz from an offshore tower. In the range 5 to 30 Hz their results appear to show a more or less uniform wind speed dependence of spectral levels, with saturation at wind speeds above approximately 15 ms^{-1}.

LLEONART and BLACKMAN (1980) studied wind-generated capillary waves in a wind-wave channel and concluded that the range over which surface tension was predominant (from 15 Hz up to f_v) could be described by a displacement energy spectrum of the form:

$$E(f) = D.u_*^2(u_*v/\gamma)^{1/2}f^{-3}$$

where D is a constant and v is the viscosity.

Some uncertainty may exist as to the calibrations, particularly in terms of frequency response, of some of the sensors used in support of these various spectral forms. Early measurements with sensors having reduced high frequency response led to the belief that an f^{-5} law applied to higher frequencies than have subsequently been shown to conform, for example. Consequently, it is not surprising that a variety of empirical forms have been proposed for the high frequency wave spectrum. However, the comments of PIERSON (1976) on the necessity to develop a theory to account for the observations, rather than to doubt observations which do not agree with theoretical predictions, seem to be valid in this complicated situation. Or, in the words of Leonardo da Vinci, "Remember, when discoursing about water, to induce first experience, then reason".

3. ONE DIMENSIONAL MEASUREMENTS

If we consider techniques for the measurement of surface elevation, z, in a vertical line (i.e. constant x,y), these techniques can be classified very broadly as invasive (surface-contacting or -piercing) and non-invasive (remote, non-contacting).

A useful technique must be capable of providing (a) adequately fine spatial resolution, in the x,y plane, and (b) adequately short temporal resolution, in the time domain. As discussed above, the waves of interest in radar scattering are of approximately 1.5 cm wavelength (15.6 Hz) for an X-band radar operated at near grazing incidence.

Due to averaging over the sensed area of water surface, any sensor will have a limited spatial resolution. The sensed area will usually be circular in the x,y plane, resulting in a directionally isotropic response function, T(k), which can be shown (see Appendix A) to be of the form:

$$T(k) = J_0(kr) + J_2(kr)$$

for a unidirectional wave of wavenumber k and for a sensed area of radius r, where $J_n(kr)$ is the n^{th} order Bessel function. In the case of a sensor which averages the surface elevation around the periphery of a circle in the x,y plane, the response is given by:

$$T(k) = J_0(kr)$$

These expressions were derived on the assumption that the sensor response is uniformly weighted over the area, or circumference, respectively.

For a 90 percent amplitude response to waves of λ = 1.5 cm, this restricts the sensed area to a circle of approximately 0.42 cm, or 0.31 cm, diameter, respectively. Thus, as a rule of thumb, the horizontal dimensions of the sensed area should not exceed one quarter wavelength of the highest frequency waves that are to be observed.

In the case of surface-piercing sensors, the presence of the sensor will modify the wave field, due to reflection and diffraction of the waves by the sensor and any associated supporting structure. The importance of such effects will depend upon the dimensions of the sensor, relative to the incident wavelength, and upon whether the sensor is fixed (as in the case of a wave staff) or free to move (as in the case of a float). Surface piercing objects will also generate waves by converting flow energy into wakes, vortices, etc., as discussed below. The continued use of surface-piercing sensor techniques, in the face of these problems (and others, yet to be mentioned), is due to the simplicity of direct sensing as opposed to remote sensing devices, both in practical realisation and in use.

4. DIRECT (SURFACE-PIERCING OR CONTACTING) H.F. WAVE SENSORS

4(a) Wave Staffs

The wave staff, in resistance wire or capacitance wire form, has been used in a number of investigations of the high frequency end of the gravity wave spectrum and into the capillary wave spectrum, in addition to the more usual applications at lower frequencies. Such investigations have mainly taken place in wave or wind-wave tanks, although lakes and reservoirs have also been used. For practical reasons, as will become apparent, a wave staff designed to measure water surface waves of greater frequency than, say, 4 Hz can only cover a limited range of displacement. Therefore it is not, in general, practical to make a high frequency wave staff which will cope with open sea conditions.

This can, however, be achieved if it is mounted on a platform which follows the sea surface motions over most of the gravity wave spectral range, such that residual motions of the surface relative to the platform do not exceed the wave staff range. This approach has been adopted by BAKER (1970), who used an array of wave staffs mounted on a modified pitch-roll buoy to measure wave directionality at high frequencies. High frequency wave staffs, as well as air flow and pressure sensors, have also been deployed on mechanisms which are servo controlled to follow the lower frequency, large amplitude, vertical excursions of the water surface. Examples of such devices are given by SHEMDIN and HSU (1967), CHANG *et al.* (1970) and by SHEMDIN and TOBER (1980), amongst others.

In connection with such wave followers it is worth mentioning that a non-contacting surface follower with high frequency response, based on a moving coil (loudspeaker type) actuator, with a capacitance probe surface separation sensor was made in connection with studies of wave power conversion techniques. The capacitance sensor used a small electrode on the bottom of the moving platform; the (very small) capacitance formed between this electrode and the water surface was measured and compared with a set value so as to provide an error signal for the servo. Due to fringing fields, the effective susceptance of the probe is not a simple linear average of the vertical separation over some effective area. Consequently, the vertical displacement of the device is a somewhat distorted version of the vertical surface displacement. It is possible that improved linearity could be achieved by the use of a guard ring around the moving electrode.

The performance of a wave staff in the high frequency range suffers from a number of problems which can be grouped under the headings of a) effects due to the meniscus at the probe/water/air interface and due to probe surface wetting, and b) effects due to interference with the water surface. Before considering these problems, it is instructive to re-examine the sensing techniques used in the two types of wave staff.

4(a.1) The resistance wire wave staff

In the case of the resistance wire wave staff a probe is constructed in such a manner that it has an (ideally) constant resistance per unit vertical height, R. This may be achieved by using a straight, vertical length of high resistivity wire, or by winding a length of resistance wire at a precise pitch on a cylindrical former with its axis vertical, as in Figures 5a, 5b. In the latter case a plastic former is commonly used, so that the wire beds in, giving a relatively smooth surface which will not entrain water. The probe is mounted with approximately equal proportions above and below the mean water level. If the water has sufficiently high conductivity, such that the effective shunting resistance due to the water, r, is much less than R, the nett resistance R_{nett} will vary linearly with water level.

$$R_{nett} = R(L-h) + \frac{R.h.r.h}{R.h+r.h}$$

$$= R(L - \frac{h}{1+r/R})$$

where L is the total length of the probe and h is the depth immersed.

The sensitivity, being dependent upon r/R, will vary with the temperature and salinity of the water.

If a constant current, i, is passed through the probe, the sensitivity in terms of the voltage, V, developed across the probe is given by:

$$\frac{dV}{dH} = \frac{i.R}{1+r/R} \text{ volts/metre}$$

The value of R, for wire of resistivity ρ_m ohms/metre and of diameter 2a, wound with pitch 4a on a former of diameter 2b, is given by:

$$R = \frac{\rho_m(b+a)}{2.a^3} \text{ ohms/metre}$$

whilst the shunting resistance due to water of resistivity ρ_w is given by

$$r = \rho_w.Fn(b+a) \text{ ohms/metre}$$

where Fn(b+a) is a function of (b+a). Strictly, r is also a function of position up the probe, due to end effects. The end effects can be considered constant if an adequate length of probe is immersed, so that r is independent of h.

For high frequency wave measurements the simple straight wire form of construction is more suitable (smaller cross-sectional dimensions in terms of wavelength and more consistent water meniscus performance). This results in a value of R given by:

$$R = \frac{\rho_m}{\pi a^2}$$

where 2a is the diameter of the wire. In order to avoid problems due to polarisation effects, an alternating current of frequency greater than about 500 Hz must be employed. However, at high frequencies, skin depth increases the effective value of r.

An alternative approach to the single resistive wire probe is the twin wire probe (FRYER and THOMAS, 1975), shown in Figure 5c. In this device, two vertical, parallel, low resistance wires are partially immersed in the water. Neglecting end effects, which can be considered to be constant if fluctuations in the immersed depth are small in comparison with the mean value, the resistance between the wires is inversely proportional to the product of the immersed depth and the water conductivity. Thus, with a constant voltage across the wires, the current flowing is directly proportional to the immersed depth. The calibration is clearly dependent upon the water conductivity and can be measured in situ.

ALTMANN (1980) describes an instrument of this type incorporating a separate conductivity cell; this is used to derive a drive voltage for the probe that is inversely proportional to the conductivity, so that the probe current is independent of conductivity. The twin wire probe will have a frequency response that is a function of wave direction. For long-crested waves propagating normal to a line joining the two wires, the response will be more or less identical to that of a single wire. For waves propagating in line with the wires, the response will be reduced by a factor cos(ks/2), where k is the wavenumber and s is the wire spacing. For example, for 4 Hz waves, with s = 1 cm, cos(ks/2) = 0.95, reducing to 0.31 at 10 Hz.

4(a.2) The capacitance wire wave staff

The concept of the capacitance type of sensor is also simple. A length of wire or rod, with a dielectric sheath, is held vertically in the water (Figure 6a). The capacitance, C, between the wire/rod and the water - which forms the outer, grounded, electrode - is given by:

$$C = \frac{k_o k . 2\pi h}{\log_e(b/a)}$$

where k_o is the permittivity of free space
k is the permittivity of the dielectric sheath
$2a$ is the diameter of the wire/rod
$2b$ is the diameter of the sheath
h is the immersed depth

The potential of the outer electrode is normally sensed by means of a connection to the metallic supporting structure used to tension the wire, assuming that the impedance of the water path from this to the outer electrode is negligible in comparison with the reactance of the capacitor so formed. The variation of the capacitance with h can be converted to a useable electrical voltage in a

number of ways: one method is to measure the current, i, through the probe when it is connected to an alternating voltage source V.sin(2π ft)

$$i = \frac{4\pi^2 k_o k f}{\log_e(b/a)}.V\cos(2\pi ft)$$

$$\sim h.\frac{4\pi^2 k_o k f a}{t}.V\cos(2\pi ft)$$

if t<<a, where t (=(b-a)) is the thickness of the dielectric sheath.

Another method is to use the capacitance to set the pulse length, T, of a monostable flip-flop which is triggered at a constant rate, f, where f>>highest wave frequency to be observed.

e.g. if T = K.C, the the mean voltage, v, of the monostable output (logic levels V(high), 0(low)) is given by:

$$v = TfV$$

$$= \frac{2\pi K k_o k f a V}{t}.h$$

In practice, C will have associated stray capacitance which, if constant, merely offsets the output - of little importance to wave measurements - and series resistance, which results in non-linearity.

4(a.3) Other Types of Wave Staff

Various other types of sensing techniques have been used, including sensors with "digitised" outputs resulting from the use of a large number of discrete electrodes at uniform vertical spacing up the staff. These are not relevant to the present study since they lack the required vertical resolution for high frequency measurements. Another technique, which has been used successfully for the measurement of gravity surface waves, is the microwave transmission line technique. One form used a length of microwave waveguide supported vertically in the water. The waveguide was slotted with slots of smaller dimensions than the microwave wavelength, so that the water level inside the waveguide could follow the outside level up to some frequency determined by the hydraulic filtering effects of the slots; the microwave energy could not, however, leak out through such slots. Pulses of microwave energy were transmitted from the upper end of the guide down to the air-water interface, where almost all of the energy was reflected. The skin depth of water at microwave frequencies is of

the order of a mm. Water level was determined by measurement of the two-way transit time of the microwave pulse, i.e. by time domain reflectometry. The height resolution achieved was determined by the bandwidth of the microwave system and by variations in water level over the cross section of the waveguide due to water slopes and meniscus effects at the waveguide walls. The frequency response in terms of the water waves would be determined by the cross-sectional dimensions of the waveguide (spatial filtering) and by the hydraulic filtering effects. The combination of meniscus and hydraulic filtering effects and of the high time resolution required to give adequate vertical resolution (e.g. 0.7 picoseconds for 0.1 mm) render this type of sensor and detection system an unlikely candidate for the measurement of high frequency surface waves.

FISCELLA et al. (1982) and TRIVERO and CAPPA (1987) have, however, reported a modification of this technique which, they claim, has a response up to a wave frequency of 26 Hz and an accuracy in height of 42 microns. They used a "Goubau line", as shown in Figure 6b, consisting of a teflon-coated wire (surface waveguide), of overall diameter 1.8 mm, as the microwave transmission line. The phase of the X-band standing wave pattern due to the X-band wave reflected from the water surface was measured using two detectors electricallly spaced by $(2n+1)\lambda/8$. If the phase is computed from these detector outputs at close enough intervals, the water surface elevation can be tracked over a range of many X-band wavelengths. The upper frequency limit quoted is equivalent to a water wavelength of twice the effective diameter of the probe (an area of this diameter about the probe contains 50 percent of the X-band surface guided wave power). The vertical accuracy results from a microwave phase measurement accuracy of 1°. Doubts must, however, be expressed regarding the performance of this system at high surface wave frequencies, because of skin depth and meniscus complications.

4(a.4) General High Frequency Performance of Wave Staffs

The above sections 4.a.1 to 4.a.3 summarise the basic wave staff techniques. Of prime interest in the present study is the dynamic response of the wave staffs. Apart from fundamental spatial filtering effects due to the physical cross-sectional dimensions of the devices, treated in section 3.1, the main limitations in practice are due to the behaviour of the water meniscus at the probe-water-air interface and associated wetting of the probe surface; such wetting can extend to an appreciable distance above the level expected from a static meniscus.

The wetting is due to a combination of surface tension, allied to the nature of the probe surface, and to the high apparent downward accelerations experienced by water particles in the vicinity of the probe at the crests of steep gravity waves. LONGUET-HIGGINS (1986) has shown that the apparent downward acceleration of the water surface in a fixed vertical line exceeds 1'g' for waves

of steepness ak>0.33 (where a is peak amplitude and k is wave number = $2\pi/\lambda$). This steepness is less than the value of ak = 0.4432 for gravity waves of limiting steepness. The significance of this is that, in a wave of quite moderate steepness, a water particle constrained to slide down the wire, rather than follow the orbital motion, would be "left behind" above the retreating water surface. It is reasonable to suppose that this would apply to water particles in the immediate vicinity of the probe surface, resulting in the temporary existence of a water film above the retreating surface.

Additionally, the surface of the probe will almost inevitably become contaminated both by adsorbed water, organic fluids and gases and by surface films. Both types of contamination will affect wettability and meniscus behaviour, resulting in unpredictable hysteresis in the probe response. A major cause of such hysteresis is"meniscus flip", which occurs in some surface/fluid combinations. This results in the contact angle (Figure 7) between the meniscus and the probe surface flipping between two, approximately stable, values according to the sign of the water level velocity relative to the probe. e.g. with falling water level, the contact angle might be 30° and with rising water level the contact angle might be 150°. This would cause flattening of the sensed wave crests and troughs, giving odd order harmonic distortion and a phase lag at the wave frequency.

Apart from dynamic considerations, the meniscus increases the effective diameter of the probe from the point of view of spatial filtering. WHITE and TALLMADGE (1965) carried out accurate measurements of the profiles of static menisci on the outside of cylinders immersed in a fluid. The contact angle of the meniscus with the cylinders was zero (perfect wetting, ensured by addition of a wetting agent). STURM and SORRELL (1973) carried out measurements on the response of a resistance wire probe of 0.224 mm diameter, relative to results derived from an optical slope gauge (using linear theory to convert slope to displacement). The effective diameter necessary to account for the reduced response of the resistance wire sensor by spatial filtering was found to be 5-7 mm. This amounted to the diameter of the (static) meniscus profile at which the height of the water surface was 1/10th of the total meniscus height, as measured from the undisturbed level. They explained the reduction in probe response at high frequencies in terms of spatial filtering over the effective diameter of the probe resulting from the extent of the meniscus (Figure 7). It seems unlikely that static meniscus profiles are maintained in the case of rapid fluctuations of level and in the presence of surface slopes, even in ideal cases where there is no surface contamination.

SPINDEL and SCHULTHEISS (1971) reported an investigation using capacitance wire wave probes constructed from Formar-coated 40 a.w.g. wire. The response of these probes was measured, by vertically vibrating them in still water, to be flat to over "100 Hz/inch", spatially, which seems improbable.

KONDO *et al.* (1973) used a 0.3 mm diameter copper wire with a synthetic resin coating to investigate the wind speed dependence of the h.f. wave spectrum. They quote a "response time" of 30 milliseconds for this capacitance probe.

LLEONART and BLACKMAN (1980) used fine enamelled wire capacitance wire wave probes, of overall diameter 50 to 100 microns, for measuring displacement and slope (by means of a two-wire differential probe with 0.5 mm spacing). They reported reliable operation provided that the probes were soaked for an adequate time before use. High speed cinephotography revealed no obvious meniscus problems.

HENDERSON and HAMMACK (1987) have reported that the use of glass as a dielectric for capacitance wire wave probes removes the problem of meniscus flip but, since glass adsorbs water and other contaminants to a significant extent, their results may not be applicable to long term use under other than laboratory conditions. The water used in their experiments was filtered through 0.2 micron filters and the wave tank was covered so as to reduce surface contamination. Any such contamination would affect the surface waves in the gravity-capillary and capillary ranges, apart from contaminating the probe surface itself.

LOBEMEIER (1981) has reported the successful use of fine tungsten wire in an essentially resistive wave probe at wave frequencies of 50 Hz or more. The diameter of the tungsten wire used in "small" waves was only 40 microns, whilst for waves of up to 2 metres in height the wire diameter was increased to 0.5 mm. A special calibration system was produced to evaluate the frequency response. This included a wedge plunger type of wavemaker, which could generate waves of up to 50 Hz, and an optical height measuring system. The latter used the coincidence of light transmission along two separate paths, to measure the height of horizontal reflecting wave facets; a resolution of 5 microns in height was obtained. The response appears to have been uniform up to the highest frequency of the wavemaker. The success of this sensor is thought to have resulted from the very small diameter of the wire used. According to the work of STURM and SORRELL (1973), the effective diameter for Lobermeier's 40 micron wire would be approximately 1.5 mm, resulting in 90 percent probe response at a wave frequency of 49 Hz.

In general, resistance wire probes have been found to be superior to capacitance wire probes for the measurement of high frequency waves. This is mainly due to the problems in making a reliable, small diameter, capacitance sensor; dielectric contamination/deterioration are significant problems.

Apart from possible dynamic response limitations, problems inherent in the use of wave staffs for the measurement of high frequency waves include vibrations of the staff, effects of the staff on the

water surface and the possibility of motions of the platform supporting the staff, as detailed by KUO and GROSCH (1972). A wire under tension with its bottom half in water can be excited by flow past the wire. This can result in the generation of capillary waves/vibration and eddy shedding at the Strouhal frequency, given by:

$$f = 0.2\frac{u_o}{d}\left(1 - \frac{19.7v}{u_o d}\right)$$

where u_o is the speed of flow past the wire

d is the wire diameter

v is the kinematic viscosity, $\sim 10^{-2} cm^2 sec^{-1}$

giving $f = 46$ Hz for a wire of 1 mm diameter

$f = 106$ Hz for a wire of 0.1 mm diameter.

A capillary wave of frequency 46 Hz has wavelength $\lambda = 0.63$ cm and a phase velocity $c = 29.0$ cm/sec. Waves will be generated when the flow rate past the probe is greater than the minimum wave phase velocity c_m (23.0 cm/sec). In open sea conditions, the flow past the probe will be due to tidal and wind-driven surface currents and to the orbital velocities of longer surface waves.

KUO and GROSCH consider wave orbital velocities alone, and derive a critical wave amplitude, a^*, given by

$$a^* = c_m \cdot \frac{\lambda}{2\pi g}$$

above which the orbital velocity will instantaneously exceed c_m twice per cycle. They then calculate that for a Phillips' saturation equilibrium spectrum (f^{-5}) this will occur for wavelengths greater than 2.5 metres. Thus one would expect a wave staff to generate capillary waves during at least part of the time under open sea conditions.

Another problem due to relative flow is that water tends to build up at the leading edge of the probe and to be depressed at the trailing edge. Since such level changes are dependent upon the instantaneous flow rate, one might expect errors at the wave frequency. However, since flow rate is proportional to f^{-4} whilst amplitude is proportional to $f^{-2.5}$, this is not so much of a problem at high wave frequencies.

If the platform upon which the probe is mounted moves with the lower frequency waves (λ>0.5 metre, say), the generation of waves by the probe itself is unlikely. However, waves generated by the platform, and modification of the wave field by the platform, are other likely sources of considerable error. Additionally, vibrations of the platform can be caused by, for example, wave slamming, flow instabilities, etc.

A further possible cause of probe vibration is excitation by wind flow past the length of the wire exposed in air. The wire, normally under tension, will have resonances whose frequencies and damping are dependent upon the water level.

4(b) Surface floating devices

One of the most common techniques for the measurement of surface waves having wavelengths longer than about 2 metres is to measure the motions of a surface-following buoy; the Datawell Waverider is an example of this technique. The surface-following buoy is not normally a perfect particle follower, unless it is allowed to drift freely (with the Stokes' drift). A compliant mooring is normally used which results in a limited horizontal range of motion; the moored buoy is, therefore, neither a true Eulerian nor a true Lagrangian sensor. Consequently, a certain amount of spectral translation of apparent energy occurs, as described by LONGUET-HIGGINS (1986); this is normally overlooked or neglected.

It has also been suggested by BARSTOW (1985) that some combination of types of surface buoy/mooring result in the buoy "skating round" surface features such as pyramidal (short crested) waves. Also, the surging motion of the buoy on the compliant mooring results in reduction of the asymmetry of the profiles of extreme waves (sharp crests/smooth troughs), giving an artificially low skewness of the surface displacement distribution.

The possibility of producing a miniature surface following buoy and associated mooring/tethering system, which could be used to measure high frequency waves in a wind/wavetank or reservoir, has been considered. This would have some advantage over other surface-piercing (e.g. wave staff) techniques in that meniscus and allied effects would be of lesser importance. However, unless the device was completely free drifting, motion relative to the water particles (and consequent effects similar to those described in 4.a.3, above) would still occur. The practical problems involved in measuring the motions of a surface follower of, say, 5 mm diameter would be severe. Such a device could be fitted with an unstabilised "apparent vertical" accelerometer, using state-of-the-art silicon sensor technology. Signal and power connections to the surface follower would have to be via fine

electrical ligaments. A miniature accelerometer buoy of 10 cm diameter was constructed in connection with the measurements described by LONGUET-HIGGINS (1986).

Another possible approach might be to remotely sense the motion of the surface-follower, using it as a surface marker. This would be more reliable than attempting to remotely sense the motion of the surface itself, for reasons which will be made clear in Section 5, below. One possibility, for example, is that the motions could be sensed using a number of video cameras using digital scanning (charge-coupled devices) and some form of intelligent image processing system. Acoustic tracking of the float is another possibility. The principal difficulties foreseen are the reliable recognition of the object (float) and the achievement of sufficient positional resolution over an adequate 3-dimensional dynamic range. A resolution of 0.1 to 0.2 mm in the vertical position would be desirable.

A more promising approach might be to use an x,y position sensing system (e.g. ccd camera) to sense the position of the float in a horizontal image plane (the float could be painted orange or yellow to aid recognition). This position would then be used to compute the beam deflections, θ_x and θ_y, necessary to direct a narrow laser radar beam at a small corner reflector, fitted centrally in the float with its apex at the water level. The centre of pitch and roll motions of the float should, ideally, coincide with the corner reflector apex. The vertical (z-axis) position of the float could then be derived from the radar range, R, and from the beam angle from the vertical, θ,

$$\text{where} \quad \theta = (\theta_x^2 + \theta_y^2)1/2).$$
$$z = R.\cos\theta - z_o$$
$$\text{i.e.} \quad dz = -R.\sin\theta.d\theta$$

so that, if the maximum horizontal excursion of the float from the laser vertical axis, $R\sin\theta$, is 2 cm (applicable for waves up to about 20cm wavelength), the beam must be aimed to an accuracy of 10 mrad for 0.2 mm error in vertical position of the float, dz. If R was made to be 2 m, or more, the maximum beam deflection would be 10 mrad or less. Consequently, the required accuracy could be achieved with a fixed beam of rather more than 10 mrad beamwidth, provided that no problems arose from sporadic specular reflections within the illuminated area competing with the return from the corner reflector. Small angle laser beam deflection at frequencies up to several tens of Hz could be achieved by means of mirrors mounted on piezo-electric flexural elements. The x,y positional information could also be used to compute the directional wave spectrum.

The time resolution necessary to achieve 0.1 to 0.2 mm height resolution (0.67 to 1.34 picoseconds) is not practically attainable. An interferometric (fringe-counting) technique would be necessary. For the above surface wavelength range the maximum float velocity in the laser boresight

direction will be approximately 25 cm/s, resulting in a maximum fringe counting rate of 790 kHz for a 0.633 micron laser: this is not excessive. However a fringe counting system would be considerably upset by any stray returns (e.g. specular reflections) of amplitude comparable to, or greater than, the corner-reflected signal. It would seem preferable to incorporate the complexity of steering a narrow (of diameter less than the corner reflector) laser beam rather than use a wide fixed beam with the attendant problems of stray returns.

The type of sensing system outlined above would only be suitable for use in wavetanks or in limited wind/fetch situations. It would be expensive, but it would be capable of producing directional information. The limitation on frequency response would arise from practical limitations upon the size of the surface following float and its tethering system. The frequency response of the beam steering devices should not be a limitation, certainly for waves of less than 50 Hz. If the range R was made to be 2 m, such that θ is in the range 0 to ~0.01, no correction for slant range would be necessary; the vertical displacement would be simply proportional to the count in the up/down fringe counter, which could be converted to an analogue signal, or logged directly. The horizontal x and y displacements would be simply proportional to the voltages applied to the beam deflectors. A schematic of such a sensing system is shown in figure 8.

5. INDIRECT (REMOTE OR NON-CONTACTING) H.F. WAVE SENSORS

5(a) Optical Techniques

Optical techniques which have been used for direct sensing of the water surface, rather than a floating marker as proposed above, fall into two main categories: these are surface displacement/velocity measuring systems and surface slope measuring systems. The former category includes laser radars (lidars), doppler velocimeters and anemometers (using interference fringe fields). The latter category includes devices (again mostly incorporating lasers) using refraction or reflection at the sea surface to measure the slope of the water-air interface - usually in two orthogonal planes including the vertical.

5(a.1) Surface Displacement/Velocity

Instruments for the measurement of surface displacement by optical techniques have relied upon the reflection or backscattering of energy at the water-air interface. Normally, in the absence of surface features such as foam or floating particles, the actual water-air interface will have no features capable of scattering (size comparable to, or less than, the wavelength of the light waves). Consequently, the light waves will be purely reflected and refracted in the proportions given by Fresnel's equations (see, for example, SMITH 1960):

$$\frac{A_{reflected}}{A_{incident}} = \frac{\tan(\theta_1 - \theta_2)}{\tan(\theta_1 + \theta_2)}$$

$$\frac{A_{transmitted}}{A_{incident}} = \frac{2\cos\theta_1 \sin\theta_2}{\sin(\theta_1 + \theta_2)\cos(\theta_1 - \theta_2)}$$

- for vertically polarised light waves

and

$$\frac{A_{reflected}}{A_{incident}} = -\frac{\sin(\theta_1 - \theta_2)}{\sin(\theta_1 + \theta_2)}$$

$$\frac{A_{transmitted}}{A_{incident}} = \frac{2\cos\theta_1 \sin\theta_2}{\sin(\theta_1 + \theta_2)}$$

- for horizontally polarized light waves, where θ_1 is the angle of incidence and θ_2 is the angle of refraction, related by Snell's law:

$$\sin\theta_1 = n.\sin\theta_2$$

n being the refractive index of sea water.

The reflection coefficients are shown in figure 2. For values of $\theta_1 < 30°$ (the range which would apply for a vertical light beam incident upon the water wave surface), the amplitude of the reflected light is more or less constant at about 0.14 of the incident amplitude; in terms of intensity, this amounts to about 2 percent.

This has two serious implications: the first is that the illuminating beamwidth must be greater than the maximum spacing of horizontal reflecting facets on the water surface to ensure a return. The second is that a relatively large return may result from backscattering from particles below the surface (bubbles, plankton, etc.), since most of the energy is transmitted through the surface for the above range of θ_1. In laboratory experiments, it is possible to artificially "seed" the water surface with optical scatterers. In trials of a Laser Doppler Velocimeter (LDV) described by EWING *et al.* (1984), glass microspheres (of the type used as a filler in syntactic foams for deep buoyancy) were successfully used for this purpose. Interestingly, these microspheres have also been used quite independently by MELVILLE and RAPP (1988), who also suggest the use of white latex paint; the latter tends to disperse vertically, however. They also used dye to attenuate light transmitted into the water, so as to reduce subsurface backscattered intensity.

Laboratory techniques may not be transferable to the open sea or even a reservoir, as was found with the LDV. The seed particles drift down wave with Stokes' drift, so that continuous seeding was necessary to maintain an adequate population within the light beam. This seeding was not easily achieved in other than light winds, since the particles simply blew away if attempts were made to drop them from a hopper above surface. A subsurface distributing system could, perhaps, have solved this problem but sufficient time was not available to attempt this. Breaking waves were also a cause of particle dispersion, resulting in intermittent signal loss.

The Laser Doppler Velocimeter (Figure 9) measures the Doppler shift (f_d) of the frequency of the transmitted coherent laser beam after reflection or backscattering by the "target", giving a measure of the velocity of the target in the direction of the beam axis. In order that both positive and negative velocities may be measured, the transmitted beam is offset in frequency from the reference beam, with which the return is heterodyned, by a frequency f_b; this shift is achieved by means of a Bragg cell. The heterodyned output at $f_b + f_d$ is then heterodyned again (in the Disa system evaluated by IOS) with a frequency $f_b + f_o$, giving an output at $f_o - f_d$ which is tracked and converted to an analogue voltage by a phase-locked loop with a selectable tracking range of $0.1f_t$ to f_t.

The frequency offset f_o is set to be greater than the maximum expected value of f_d and the tracking range f_t is set to approximately $2.f_o$, so that $f_o - f_d$ remains within the range $0.1f_t$ to f_t at all times. The actual phase locked loop frequency ($f_o - f_d$) or the analogue output voltage (given by $10.(f_o - f_d)/f_t$ volts) can be logged. The Doppler shift f_d is given by:

$$f_d = 2.\frac{v}{\lambda} = 2.\frac{v}{c}.f$$

where v is the component of velocity towards the laser (ms^{-1})
c is the velocity of light in air
f is the optical frequency
λ is the optical wavelength

for the Helium-Neon laser operating at a wavelength of 632.8 nanometres, $f_d = 3.161v$ (MHz).

Typical "significant velocities" in the wavetank and reservoir trials were in the range 0.05 to 0.30 ms^{-1}. The LDV electronics system, as tested, may not have been optimally set up for this type of application; severe problems were initially experienced in maintaining phase lock in wave tank trials. These appeared to be due to the wide dynamic range of the return signal level although, to a human

observer, this did not seem excessive. It is also possible that returns from the water surface and from particles below the surface varied in relative intensity in such a manner as to confuse the loop.

Various seeding additives were tried, including milk, paint, aluminium powder and the glass and ceramic microballoons referred to above. The particles in milk and in paint (TiO_2) scattered the laser beam well but dispersed rapidly, giving an unreliable target depth. Aluminium powder was quite successful in the wave tank. However, since it relied upon surface tension to keep it "afloat", it was difficult to achieve a reliable uniform coating of the water surface.

The glass and ceramic microballoons were the best seeding material, glass being slightly superior due to lower absorption losses. Ceramic microballoons were, however, used on account of their much lower cost (1/10th that of glass). The microballoons used in the trials had diameters in the range 50-175 microns, with typical wall thickness of 3.5 microns. The true mean density of the microballoons was 0.6. The Stokesian response time T_s for a particle of radius a with mean density ρ_s in a fluid of kinematic viscosity v and density ρ, is given by:

$$T_s = \frac{2a^2}{9v} \cdot \frac{\rho_s}{\rho} - 1$$

For a = 50 microns and $\rho_s = 0.6$, $T_s = 222$ microseconds, which is negligible compared with the wave periods of interest.

The microballoons result in returned light partly due to backscatter, but mainly due to multiple internal reflections; there is, thus, some possibility of effective range errors but, due to the large number of spheres within the laser beam at any time, these do not appear to have been important.

The problems experienced in using the microballoons have been mentioned above. A further difficulty, experienced in all except low winds, was a tendency for the balloons to be dispersed by breaking wavelets. Another cause for concern was whether the presence of the microballoons in such large concentrations affected the behaviour of the surface waves under study. All in all, the method was not considered to be very satisfactory.

The measurements carried out by MELVILLE and RAPP (1988), used a quite different laser technique, that of Laser Doppler Anemometry (LDA). In this technique two beams, derived from a single laser of wavelength λ, are projected so as to cross at a small angle, θ. Interference fringes result over the (roughly ellipsoidal) beam crossing region. Planes of maximum intensity occur at spacings of λ_x in the direction, x, normal to the bisector of the two beam axes (in the plane containing the two

beam axes). This is easily shown by considering the sum of the amplitudes of two beams (frequency ω, wave number k) propagating in the xy plane at angles of $\pm\theta/2$ to the y axis.

$$\text{Sum of amplitudes} = a.\cos(\omega t + kx.\sin(\theta/2) + ky.\cos(\theta/2)) + a.\cos(\omega t - kx.\sin(\theta/2) + ky.\cos(\theta/2))$$

$$= 2a.\cos(\omega t + ky.\cos(\theta/2)).\cos(kx.\sin(\theta/2))$$

The intensity therefore has maxima when $kx.\sin(\theta/2) = N\pi$,

$$\text{i.e. when } x = -\frac{N\lambda}{2.\sin(\theta/2)} = N.\lambda_x$$

$$\text{giving } \lambda_x = \frac{\lambda}{2.\sin(\theta/2)}$$

The passage of a scattering particle across this region in the plane normal to the beam axis bisector will, if it is smaller than about half the fringe spacing λ_x, result in backscattered light which is modulated in intensity at a frequency, f, which is given by:

$$f = v_x/\lambda_x$$

where v_x is the velocity component of the particle in the x direction.

For small angle θ,

$$f \sim v_x.\theta/\lambda$$

For example, if $\theta = 1°$, the resulting fringe spacing λ_x, for the He-Ne laser optical wavelength of 633 nm, is 36 microns, giving a fringe crossing frequency, and hence intensity modulation frequency, f, of 27.6 kHz per metre/sec.

A consideration of some importance is that the received signal intensity is inversely proportional to the square of the distance of the scattering particle from the receiving lens. The beam crossing zone, constituting the actual sensing volume, measures approximately D by D/θ (for small θ), where D is the focussed beam diameter. Melville and Rapp achieved a zone of 6 cm height with the optics of the vertical axis LDA with which they measured a horizontal component of wave velocity. Horizontal velocity was required for their studies of breaking waves but, unfortunately, it cannot be used to infer vertical velocity or displacement for other than linear (low steepness) waves.

It appears to be impractical to use fringe techniques for measurement of vertical particle motion at a water-air interface. This would require beams at angles of $\pm\theta/2$ to the horizontal, i.e. one beam, would have to propagate through the water, with consequent problems. Furthermore, the minimum practical value of $\theta/2$ would have to exceed 30° if shadowing by waves were not to occur; the resulting fringe spacing would be, at most, equal to the optical wavelength. This would necessitate the use of submicron scatterers with consequent poor signal/noise ratio. The useful sensing volume would also be undesirably wide, resulting in an unacceptable degree of spatial filtering of the water waves.

Apart from laser devices employing the Doppler effect and fringes, as described above, surface displacement can be sensed by optical radar (lidar). A number of devices have been developed for this purpose. IOS participated in trials of a Spectra-Physics Geodolite 3A laser altimeter, flown in a Sea King helicopter, described by PITT *et al.* (1978). This used a Helium Neon laser whose output intensity was sinusoidally modulated at a frequency in the h.f. band. The beam diameter at sea level was about 20 cm, for a helicopter height of 21 m. The phase of the modulation on the received (backscattered and/or specularly reflected) signal was compared with that of the transmitter modulation to give a measure of height of the helicopter. The vertical motion of the (hovering) helicopter was measured using a vertical accelerometer; combination of the two measurements gave the wave displacement. An extensive series of more direct wave measurements were also taken with the laser altimeter on an offshore platform. The laser system incorporated a phase-locked tracking circuit with an adjustable time constant. However, it was found that the circuit frequently lost lock. This appeared to be due to excessive signal strength fluctuations and occasional spray which effectively caused instantaneous height changes.

A more recent airborne oceanographic lidar system (AOL) was developed by HOGE *et al.* (1980). This can use either directly backscattered or laser stimulated fluorescent emission from the sea surface. A comparison of time series obtained simultaneously from the AOL, using 5 milliradian beamwidth, and from a SCR (surface contour radar), using 21 milliradian beamwidth clearly shows the distortion which results from the use of radars (or sonars) with beam diameters that are too large in comparison with the surface wavelengths.

A commercially available lidar for wave sensing is produced by EMI. This uses a semiconductor infra-red laser with conventional range measurement in terms of travel time. The EMI laser has been involved in a number of trials (e.g. CRABB *et al.* 1983); these have, again, demonstrated that spray is a problem in the interpretation of data from optical radars used above the open sea. From the point of view of the present study, a major problem is the dynamic range of the return signal, especially when the illumination is necessarily limited to a small area. The temporal

resolution needed to resolve the height of centimetric surface waves accurately is a further problem which one may reasonably expect to be ameliorated by future advances in fast circuit devices.

LIU and LIN (1982) have described a laser displacement gauge, using essentially camera techniques, whereby the air/water interface was delineated reliably by an Argon ion laser beam directed vertically down into the water; Fluorescein disodium salt was added to increase the optical contrast of the interface. A vertical self-scanned diode line array was used in a "camera" viewing the water surface from the side of the wave tank (normal to the direction of wave propagation). This gave a resolution of 1/256th of the total displacement range and a sampling rate variable between 25 and 2500 Hz.

5(a.2) Slope Measurement

Measurement of the slope of waves by optical techniques is relatively straightforward; reflection and refraction of a light beam at the air-water interface are two practicable techniques. In the former case, the light beam is usually directed vertically down on the water. A fraction of the incident energy, given by Fresnel's equations, is reflected upwards at an angle to the vertical given by twice the local (vector) slope. The angle between the reflected beam and the vertical can then be sensed, giving one or both components of slope of the wave surface. Since the slope of the water surface can amount to 30°, in the limiting case, the reflected beam can be up to 60° from the vertical, which is inconveniently large.

An alternative reflective technique is to use an extended source, such as the radiance of a clear or completely cloud-covered sky, to allow the measurement of the reflection coefficient at a particular look angle and hence to infer the surface slope. STILWELL (1974) showed that, under certain restricted conditions, the perceived intensity is approximately linearly related to the wave slope component in a vertical plane including the direction of observation. He then used optical Fourier transform techniques to derive a 2-dimensional wave number spectrum; this had a 180 degree symmetry, as one would expect.

GOTWOLS and IRANI (1980 and 1982) further developed this technique by recording a sequence of images and using the dispersion relationship so as to allow the derivation of a wavenumber-frequency spectrum. MONALDO and KASEVICH (1981 and 1982) used a similar technique, on photographic material obtained during JONSWAP, to investigate the modulation of waves in the 3 to 30 cm wavelength range by the slope of the long carrier waves; they obtained a modulation transfer function which was essentially independent of the high frequency wavelength

and had a phase of 90 degrees. That is to say the high frequency wave amplitude was maximum at one quarter of the wavelength of the carrier wave after its crest.

The refraction of a light beam (normally a laser beam) at the surface is a more convenient technique than reflection, since the refracted beam makes a smaller angle with the vertical. The beam can either be directed down through the water surface, giving maximum angles of about 7.9° from the vertical, or directed up through the surface, as in Figure 10, giving maximum angles of about 11.7° from the vertical. The relationship between the refracted beam angle, ϕ, and the water surface slope, θ is not linear, being given by:

$$\phi = \theta - \sin^{-1}(n^{-1}\sin\theta)$$

for the downward directed beam,

$$\text{and } \phi = \sin^{-1}(n.\sin\theta) - \theta$$

for the upward directed beam.

PRETTYMAN and CERMAK (1969) used a downward-pointing laser, with the refracted beam forming a spot on a subsurface screen, which they filmed. It is generally more convenient to use an upward pointing beam, since this can be achieved with an above water laser by the use of subsurface mirrors as in CHANG *et al.* (1978); the observing system is then conveniently above water. A lens is used to focus the beam at the mean water level; this both minimises the beam diameter (and hence spatial filtering) at the wave surface and reduces focussing or defocussing effects due to water surface curvature. If the position of the refracted beam is then observed at an observing plane, normal to the unrefracted beam axis, its position will be a function both of the refracted beam angle and of the water surface displacement. The latter dependence is eliminated by using a lens above the water surface, with the observing plane at its focal point. The deflection of the spot of light formed at the observing plane is then simply a function (slightly non-linear) of the water surface slope.

The spot position can be sensed in a number of ways. One method is to use a graded-wedge type of attenuator with an intensity detector, giving an analogue output (TOBER *et al.* 1973). Another method is to use photodetector arrays or a solid state video camera, resulting in an effectively digital output. Such techniques are described by, for example, LONG and HUANG (1976), CHANG *et al.* (1978), HAIMBACH and WU (1983). The technique has even been used at sea by HUGHES *et al.* (1977), who mounted a subsurface laser and above surface vidicon camera observing system on a frame which could be deployed 10 metres ahead of the ship's bow. The use of photodiode arrays or

silicon vidicons results in fast response; for example, CHANG *et al.* (1978) quote a response extending to 700 Hz.

It is apparent that the technical problems involved in optical slope sensing of high frequency waves are much less severe than those involved in optical displacement sensing, since unreliable scattering is not involved. A basic theoretical advantage of slope sensing is that the slope spectrum is whiter than the displacement spectrum, resulting in fewer problems due to noise at high frequencies and in subsequent spectral analysis. MITSUYASU (1977) actually prewhitened the displacement signal from a resistance wire sensor by double differentiation, for this reason, in his studies of waves in the gravity-capillary and capillary ranges; such an approach can not improve the dynamic performance of the sensor, of course. The slope spectrum may also be of considerable relevance in the case of remote sensing techniques. However, it is not related to the displacement spectrum in a straightforward manner, other than by the use of linear wave theory, which has limited validity in this saturated region of the spectrum.

It was noted above that, in the case of refraction of an upward-pointing light beam, the position of the beam on an observing screen can be made independent of the water surface displacement by the use of a lens. The observing screen must be at the focus of the lens, so that a beam emerging from the water at angle θ to the vertical falls upon the screen at a distance x_1 from the undisturbed beam axis, given by:

$$x_1 = f.\tan\theta$$

where f is the focal length of the lens.

If the lens were not used, the beam would fall upon the screen at a distance x_2 from the undisturbed beam axis, given by:

$$x_2 = (H - h).\tan\theta$$

where H is the distance of the screen from the undisturbed water surface and h is the wave displacement at the beam axis. This suggests that, if H were made equal to f and a beam splitter used as shown in figure 11, the wave displacement could be derived from x_1 and x_2, e.g.

$$\zeta = f.\frac{(x_2 - x_1)}{x_2}$$

Unfortunately, since wave displacement and slope are 90° out of phase, both x_1 and x_2 will be zero at wave crests and troughs; the derived wave amplitude will therefore be indeterminate at these important features. One might think it possible to overcome this problem by biassing the beam angle (prior to refraction) at an angle of at least 30° (the maximum wave slope in a limiting wave) to the vertical. Since the critical angle for a water-air interface is ~49°, this is not practicable except in the restricted case of nearly unidirectional waves, where slopes in the vertical plane orthogonal to the mean direction are small. An offset in the plane normal to wave propagation can be used without the angle of incidence exceeding the critical angle.

5(a.3) Stereophotography

Measurements of sea surface waves by stereophotography (the SWOP project) were reported by COTE *et al.* (1960); stereocameras were flown in an aircraft. The stereo pairs produced were analysed, using a stereo planigraph, giving a two dimensional array of surface elevation measurements from which the directional wave number spectrum was calculated. The resolution allowed the measurement of components with wave numbers up to 0.69 metre^{-1}.

More recently, DOBSON (1970) mounted stereocameras on the bow of a ship, covering areas approximately 6 metres square, with 60 percent overlap. These were analysed to give profiles of surface elevation at 4 mm intervals along lines at various angles. In order to improve the estimates at high wave numbers, the large low frequency carrier waves were removed from each elevation line profile by subtracting the surface elevation obtained by a inverse transform using the 10 lowest harmonics in the complete wave number spectrum. The residual (effectively high pass spatially filtered) elevation profiles were then spectrally analysed to give wave number spectra covering the range 16 to 785 metre^{-1}.

BANNER, JONES and TRINDER (1989) have carried out stereophotography from a mean height (determined acoustically) of 6 metres. Their analysis extended to a wavenumber of 40π metre^{-1}. Considerable modulation of the energy at 19.5 metre^{-1} (1 metre wavelength) by long waves was observed.

The 180 degree ambiguity in direction of propagation inherent in instantaneous 2-dimensional measurements can be resolved by taking a rapid series of measurements and by using the dispersion relationship, as described by GOTWOLS and IRANI (1980).

5(b) Non Optical Techniques

5(b.1) Magnetic Field Measurements

WEAVER (1965) and PODNEY (1975) have derived theoretical expressions relating magnetic field fluctuations (both above and below the water-air interface) to wave motions. These fluctuations result from induced electrical currents due to the cyclically varying components of velocity of the conducting water across the Earth's magnetic field. Unfortunately, as in the case of pressure fluctuations, these magnetic field fluctuations suffer from exponential attenuation with distance from the water surface of the form exp(-kd); this is due to the resultant field being an integral of the effects over a volume. The magnetic field fluctuations below water actually increase slightly at first with depth, reaching a maximum at a depth given by $d = g/2\omega^2$ and thereafter decaying exponentially. The amplitude of the magnetic field fluctuation at the surface appears to be approximately inversely proportional to wave frequency, for a given wave amplitude. Consequently, it does not seem to be practicable to measure the magnetic fields resulting from high frequency waves when longer carrier waves are also present, unless the sensor is mounted on a structure (e.g. wave follower) which will follow the longer waves and enable a small distance to be maintained between the sensor and the surface.

5(b.2) X-ray absorption

In contrast to electromagnetic radiation at optical frequencies, soft (low energy) X-ray radiation is negligibly refracted at a water-air interface. At the wavelengths of "soft" X-ray radiation, water has an appreciable absorption coefficient, α_w, compared with that of air, α_a, suggesting that X-ray absorption might be used in measuring water level changes. Values of absorption coefficients are tabulated below for various X-ray energies, for air of density $1.204\ 10^{-3}$ g/cm^3 and for sea water of density 1.03 g/cm^3 (from KAYE and LABY (1966).

Energy	10 keV	20 keV	30 keV	100 keV
λ_{min} (nm)	$1.24\ 10^{-1}$	$0.62\ 10^{-1}$	$0.41\ 10^{-1}$	$1.24\ 10^{-1}$
α_a	$5.5\ 10^{-3}$	$7.5\ 10^{-4}$	$4.1\ 10^{-4}$	$1.87\ 10^{-4}$
α_w	$4.9\ 10^{0}$	$7.6\ 10^{-1}$	$3.7\ 10^{-1}$	$1.76\ 10^{-1}$

The X-radiation is fairly broadband, with minimum wavelength λ_{min}. If an X-ray beam of initial intensity I(0) passes through a distance, x, in air and a distance, d-x, in water, the emerging intensity I(d) is given by:

$$I(d) = I(0)\exp(-\alpha_a x).\exp(-\alpha_w(d-x))$$

$$= I(0)\exp(-\alpha_w d+(\alpha_w-\alpha_a)x)$$

The output from a logarithmic intensity detector would, therefore, be linearly related to water level.

To give some idea as to the attenuations in practice, if we take a 10 cm overall path length (d), the exponential attenuations, A(x), where $A(x) = -\alpha_w d+(\alpha_w-\alpha_a)x$, and actual intensity ratios, are tabulated below for x=4, 5 and 6 cm:

Energy	10 keV	20 keV	30 keV	100 keV
A(4)	-29.42	-4.563	-2.222	-1.057
A(5)	-24.53	-3.804	-1.852	-0.881
A(6)	-19.63	-3.045	-1.483	-0.705
I(4)/I(0)	$1.79\ 10^{-13}$	$1.0\ 10^{-2}$	$1.1\ 10^{-1}$	$3.5\ 10^{-1}$
I(6)/I(4)	$1.79\ 10^{4}$	4.56	2.09	1.42

From the point of view of maintaining linearity, the full scale ratio of intensities (e.g. I(6)/I(4)) should not be too large. Also signal strength is better for high energy X-rays. For the above dimensions (d=10 cm, x=4 to 6 cm)) x-rays of about 30 keV energy would appear to be an appropriate choice. The practicalities of generating and detecting such X-rays are another matter, as is the safety of using such a system. As an alternative to X-rays, which require bulky generation equipment, one might also consider the use of gamma radiation from a compact radio-isotope source.

The X-ray beam would have to be very narrow, to prevent spatial filtering of the waves. Any particles which came within the beamwidth would cause variations in received intensity which would be interpreted as changes in water level. Such particles are also a potential problem in some of the optical systems described above.

Absorption measurements at lower frequencies than X-rays in the electromagnetic spectrum are limited to the neighbourhood of the visible light region, where refraction at the water-air interface complicates matters, and to the low radio frequency range, where it is not possible to achieve a narrow beam of energy. Elsewhere in the electromagnetic spectrum, the absorption coefficient is prohibitively high.

5(b.3) Sub-Surface Pressure Measurements

Measurement of the sub-surface pressure field due to gravity waves has been used for many years to derive the surface displacement. The pressure at depth z (z negative below the surface) due to a gravity wave of displacement

$$\zeta = 0.5\ H \sin(\omega t - k\sin\theta.x - k\cos\theta.y)$$

is given by (LEMEHAUTE,1976):

$$p = -\rho g z + \rho g \exp(kz).\zeta$$

for the deep water case (total water column depth > π/k). Thus, there is an exponential attenuation with depth below the surface, as in the case of magnetic fields (5(b.1) above). The attenuation factor, exp(kz), is 0.00187 at a depth of one wavelength, so that high frequency pressure fluctuations are severely attenuated in even moderate depths. This has been the limitation of the method, since the attenuated upper end of the spectrum is lost in the noise level of the transducer and cannot then be retrieved by applying an inverse exponential correction function.

According to LIGHTHILL (1978), the above expression for the fluctuating component of pressure holds in the gravity-capillary and capillary ranges if g is replaced by $(g + Sk^2/\rho)$. This increases the pressure signal to be measured slightly; for a wavelength of 1 cm the increase is 3.89 times. However the amplitudes of high frequency waves are so small that the pressure signals are minute. For example, the pressure fluctuations due to a 1 mm (pk-pk) wave of 1 cm wavelength amount to 0.112 millibar (pk-pk) at 2 mm depth or 0.735 microbar (pk-pk) at 1 cm depth. The latter level, together with the necessary bandwidth (ca. 25 Hz) can be achieved with conventional (strain gauge) pressure transducers although piezo-electric sensors (hydrophones) are more sensitive. The subsurface pressure must be sensed over a small horizontal area so as to avoid spatial filtering; if necessary, this could be effected by using a water-filled, rigid-walled, truncated cone, with small apical opening, mounted on a sensor of large area.

5(b.4) Sub-Surface Particle Velocity Measurements

The measurement of two, or three, components of particle velocity below the surface has, again, been used frequently for measurement of waves in the gravity range. The most common application has been in the measurement of the directional wave spectrum, where a pressure

transducer is used in close combination of an electromagnetic or acoustic two-component current meter, measuring in the horizontal plane. The horizontal particle velocities u and v are given, in terms of a surface wave, of displacement, where

$$\zeta = 0.5\ H \sin(\omega t - k\sin\theta.x - k\cos\theta.y)$$

by $u = \omega.\ \sin\theta.\exp(kz).\zeta$

$$v = \omega\ .\cos\theta.\exp(kz).\zeta$$

There is, again, a severe attenuation with depth at high wavenumbers, due to the exp(kz) term. However, due to the ω term, the velocity spectrum is "whiter" than the pressure spectrum. Both electromagnetic and acoustic sensors have been constructed with sensor dimensions down to the order of a centimetre. It would appear to be practical to further reduce this in the electromagnetic case by use of a Helmholtz coil configuration, with one coil above water level and one below. The coil drive frequency would need to be at least twice the highest sensed wave frequency, the latter being determined by the electrode spacing.

The major problem with the pressure, current and magnetic field sensing techniques is the exponential attenuation of the signals with depth. This makes these techniques wholly impractical in situations where it is required to measure high frequency waves on top of a gravity wave spectrum, unless the sensor is mounted on a wave following platform which is servo controlled to follow the surface displacements due to the gravity waves.

5(b.5) Inverted Echo Sounders.

The measurement of high frequency waves by inverted echo sounding would require the use of a short acoustic wavelength, so that a sufficiently small area of the water surface could be insonified. In radars, echo-sounders and other ranging devices, where the shortest transit time gives the range, the beam width at the surface must be smaller than would have been suggested by considerations of simple spatial filtering. Excessive beam width results in distortion of the measured wave profile. Numerical simulations, as detailed in Appendix B, have shown that insonified surface areas of dimensions more than about 1 percent of the surface water wavelength cause significant distortion. The minimum width of a sound beam is limited by considerations of diffraction (Rayleigh limit) to the order of the acoustic wavelength, e.g. for 10 MHz ultrasound, the wavelength in sea water is approximately 0.15 mm. At this wavelength, acoustic attenuation is high (~30 dB/metre); this may not necessarily be serious, since only short path lengths are necessary unless the gravity-capillary waves

are to be measured in the presence of low frequency carrier waves. Scattering by suspended subsurface particles and bubbles is likely to be a problem in other than wave tank environments. Perversely, however, as is the case in optical radars, there may be inadequate wave surface structure with a scale small enough to cause backscattering of such short wavelength sound. The most serious limitation, however, is the lack of range resolution. If a sonar system has a bandwidth of B Hz, the best range resolution that can be achieved is given by c/B, where c is the velocity of sound in water (~1500 ms^{-1}). Since a range resolution of better than one percent of the water surface wavelength is required, the bandwidth of the transducer of the acoustic system (principally due to transducer Q) is a more serious limitation than the size of the insonified area. One would not, for example, expect to be able to measure waves of less than about 75 mm wavelength (4.5 Hz) adequately with a 10 MHz inverted echo sounder with a Q of 5.

MCILWRAITH and HAYS (1963) report the use of a parabolic reflector to achieve a narrow beamwidth at a frequency of 200 kHz. The resolutions achieved, with a transducer depth of 44 metres, were a transverse spatial resolution of 60 cm and a height resolution of 1 cm. There would seen to be limited prospects of extending the performance of echo sounders to allow the measurement of waves in the gravity-capillary region where acoustic bandwidths in excess of 10 MHz would be needed.

5(b.6) Other Techniques

There are a number of techniques for obtaining 3-dimensional information about surfaces. Moire fringe techniques have been used, but these require a surface which is a fairly uniform scatterer of light. The same constraint applies to Holography. X-ray Tomography or Nuclear Resonance (NMR) Tomography could be used to perform a 3-D analysis of a water-air interface if the sensing process could be carried out quickly enough. If the analysis were to yield useful information up to a wave frequency of 25 Hz, the complete set of data for the tomographic analysis would have to be acquired in a few milliseconds; this may be possible in the case of NMR.

6. DISCUSSION

The techniques studied almost universally suffer from restricted range; that is to say that they are not individually capable of simultaneously measuring the entire wave spectrum from gravity waves up to gravity-capillary waves. Thus, whilst there are promising techniques for measuring the gravity-capillary range in wave or wind-wave tanks or in limited areas of water such as reservoirs or small lakes, these techniques are, in general, unsuited to use in open sea conditions. Similarly, devices which are suitable for open sea use do not have the temporal or spatial resolution necessary to measure in the

gravity-capillary range. The two ranges can be covered simultaneously by mounting a high frequency sensor on a gravity wave follower, provided that the latter does not affect the high frequency wave field. Additionally, there are certain remote sensing techniques, such as stereophotography and, possibly, optical radars, which are capable of sensing different parts of the full range and could be used in parallel to achieve this.

6(a) Sensors in contact with the surface

There is little doubt that the simplicity of in-situ techniques will ensure their continued use in wave and wind-wave tank situations. The meniscus problems inherent in the use of wave staffs, in general, result in some uncertainty as to their true response. This is due to the absence of any readily available standard for comparison. The procedure adopted by a number of users for calibration, whereby the probe is subjected to known vertical vibrations while partly immersed in (hopefully) static water is inadequate. Such vibrations do not involve spatial averaging over wave slopes due to the meniscus area, which is held to be considerably greater than the cross sectional area of the wire. Additionally, the meniscus behaviour is affected by probe surface condition and water quality (contaminants), so that there is always some uncertainty as to the response except under very carefully controlled conditions.

Of the various types of wave staff, the Goubau line described by TRIVERO and CAPPA (1987) would appear to offer a number of advantages over the more commonly used resistance and capacitance wire techniques. However, since it is essentially a guided electromagnetic wave technique, in which the phase of the reflected signal is measured, small discontinuities on the line can be important. For example, if we consider a reflected signal, from the true water level, of amplitude a_1, together with an error signal of amplitude a_2, from a water droplet at height h above the true water level, i.e.

$$a_1 = \cos(\omega_S t+\phi)$$

$$a_2 = \alpha.\cos(\omega_S t+\phi-\psi)$$

$$\psi = 2\pi.h/\lambda_S$$

where λ_S is the wavelength of the electromagnetic wave on the transmission line.

The resultant amplitude, a_r, is then given by:

$$a_r = (1+\alpha.\cos\psi).\cos(\omega_s t+\phi) + \alpha\sin\psi.\sin(\omega_s t+\phi)$$

$$\sim (1+2\alpha)^{1/2} . \cos(\omega t+\phi-\psi)$$

where the phase error ψ' is given by:

$$\psi' = \tan^{-1} \frac{(\alpha.\sin\psi)}{(1+\alpha.\cos\psi)}$$

For small α, ψ

$$\psi' \sim \alpha\psi$$

The error δ in the measured water level is then given by:

$$\delta = \lambda_s.\psi'/2\pi$$

$$= \alpha.h$$

Thus, a water droplet on the line above the water level will result in an error proportional to its height above the water. This is in contrast with a resistance wire or capacitance wire gauge, where such a droplet would have no effect so long as it was not in electrical contact with the main water mass.

On the other hand, where a meniscus exists with a small angle of contact with the wire, one might suppose the resulting change in line impedance to be quite gradual, resulting in little spurious reflection of energy in comparison with the main return from the "true" water level. The error due to the meniscus might, therefore, be less than in the case of a resistance or capacitance wire sensor. Detailed investigations involving the actual sensors would be necessary to resolve these points.

In the extensive literature on the subject of resistance and capacitance wire wave staff applications, there are a number which apparently gave good results. The type of resistance wire wave staff used by LOBEMEIER (1981), in particular, appears to have possibilities for use both in tank experiments and in low sea states in the open sea.

As an alternative to fixed wave staff techniques, the measurement of the motion of surface following "minibuoys" would be technically possible. However, the necessity to moor such devices,

possibly using scaled down versions of the compliant mooring systems used on full size wavebuoys, is not attractive. They would only be useful in tank and, possibly, reservoir scale experiments.

6(b) The use of Surface-Following Platforms to support Small Scale Sensors

These devices fall into two categories: surface-following buoys, upon which small scale sensors can be mounted, as in the high frequency pitch-roll buoy work of BAKER (1970), for example, and servo-controlled platforms mounted on fixed offshore structures (towers, etc.), as described by SHEMDIN and TOBER (1980), for example. An important consideration is that the supporting platform does not unduly affect the high frequency wave field. From this point of view, subsurface systems with minimal surface-piercing components are clearly preferable. In shallow water, this can be achieved by bottom-mounted surface followers with non-contact sensing of the gravity waves by, for example, pressure sensor or inverted echo sounder. Such systems suffer from a limited range of vertical displacement, are likely to require frequent servicing and have appreciable power demands.

The "passive" solution of using a wave-following buoy as a platform upon which to mount high frequency sensors also suffers from limitations. The horizontal motions of the buoy may be undesirable; its pitch and roll motions must be allowed for and it will inevitably disturb the high frequency surface wave field due to the surface-piercing buoyancy member(s). The wide range of sea states which can be tolerated by such a system is a strong point in its favour.

The use of a non-surface-piercing capacitance probe, measuring the capacitance in air between an electrode and the surface, to provide the feedback in a surface-following servo system appears attractive but results in errors as mentioned above. The small electrode-surface spacing necessary to give adequate capacitance would make such a system impractical in spilling/breaking wave conditions.

6(c) Remote Sensors

There is no question that the measurement of surface slope by laser refraction or reflection techniques can provide accurate measurements up to the capillary wave frequency range. For some purposes slope is the required quantity but, if a displacement spectrum is required, one has to assume that linear wave theory applies, in which case the dispersion relationship can be used to convert the two component slope spectra, $\phi_{11}(\omega)$ and $\phi_{22}(\omega)$, to a displacement spectrum, $E(\omega)$, using

$$E(\omega) = \frac{\phi_{11}(\omega) + \phi_{22}(\omega)}{k^2}$$

$$\text{where } c^2 = \frac{\omega^2}{k^2} = \frac{g.\tanh(kd)}{k} + \frac{Sk}{\rho}$$

and d is the water depth.

Whilst this may be useful in the case of narrow band wave spectra in a tank, its validity in real sea conditions is questionable.

Optical methods for remote sensing of surface displacement or velocity by radar techniques have not proved to be very successful in the gravity-capillary region due to the unreliable distribution of scatterers and consequent high dynamic range of the return signal level. However, attempts to use stereophotography to measure at wavenumbers of up to 800 m^{-1} have met with some success (DOBSON, 1970), although it is not clear what accuracy has been, or can be, achieved. Such techniques may well fall down at higher wavenumbers for the same reason as the optical radars but the technique, if proven, will undoubtedly improve the understanding of high frequency wave processes in a way which is not likely to be revealed by one-dimensional sensors. There is clearly a considerable attraction in using remote techniques in this region of the wave spectrum, due to the problems experienced with in-situ (contacting) sensors.

7. RECOMMENDATIONS

Although there are applications in which a Eulerian, one-dimensional wave sensor can provide sufficient information, and there is sufficient doubt as to the performance of existing techniques to make further investigations/developments worthwhile, more useful advances in the theory of high frequency wave processes are likely to result from development of techniques for spatial observation, such as stereophotography. Such observations, in parallel with simultaneous microwave backscatter measurements from small areas of the surface (of the order of 1 m^2), in the open sea and over a range of wind speed/sea states, can be expected to yield conclusive information as to the relation between σ° and the sea surface and, with appropriate meteorological instrumentation, between σ°, averaged over a large area, and the wind speed. Such measurements would be most easily accomplished from a platform or tower in the sea, although the supporting structure of such a tower could contaminate the wind and wave fields. Measurement from a ship is another, less convenient, possibility which also poses problems of contamination. It is hoped that equipment will be procured shortly to allow tests of a short range (high resolution) stereophotographic system in a reservoir; these will be run in conjunction with measurements from relatively conventional arrays of one-dimensional sensors and meteorological sensors. If satisfactory, these tests will lead to use in the open sea. The one-dimensional measurements in the reservoir will hopefully demonstrate the errors resulting from

transformations from the frequency domain to the spatial domain, albeit in the simplified wave climate obtaining on the reservoir.

8. ACKNOWLEDGEMENTS

The author gratefully acknowledges the useful contributions made by J.A. Ewing and P.G. Challenor at the draft stage of the report.

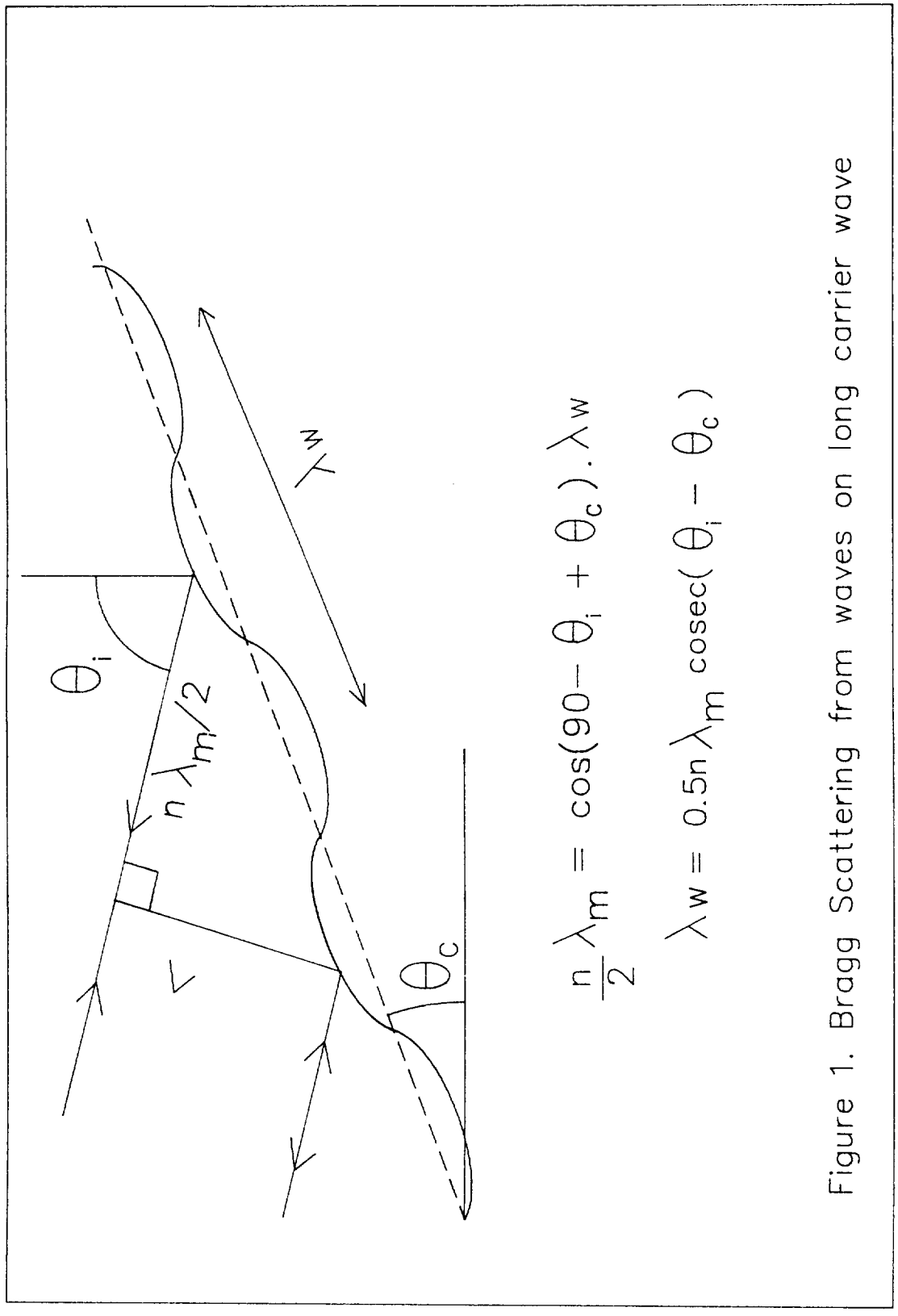

$$\frac{n}{2}\lambda_m = \cos(90 - \theta_i + \theta_c).\lambda_w$$

$$\lambda_w = 0.5n\lambda_m \operatorname{cosec}(\theta_i - \theta_c)$$

Figure 1. Bragg Scattering from waves on long carrier wave

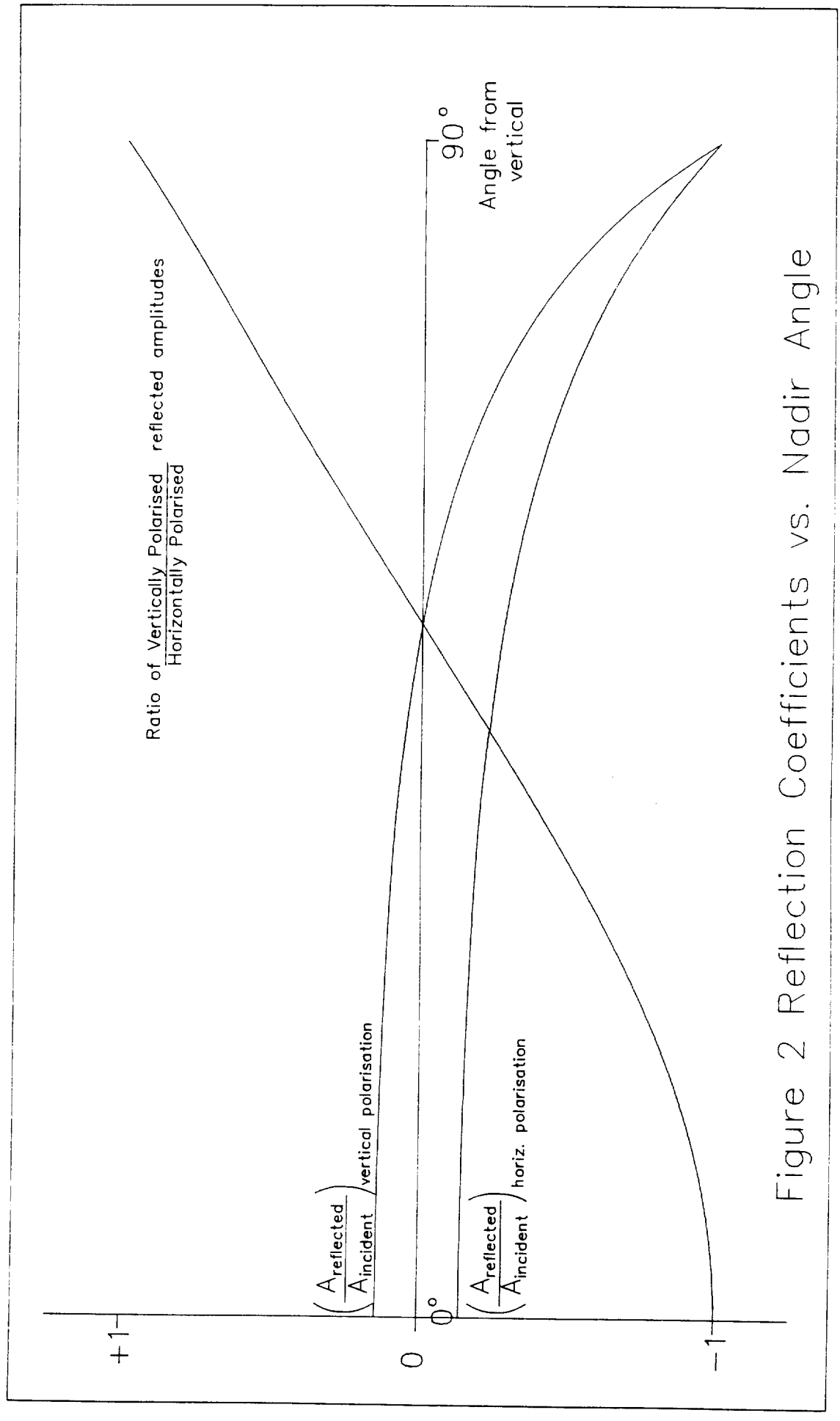

Figure 2 Reflection Coefficients vs. Nadir Angle

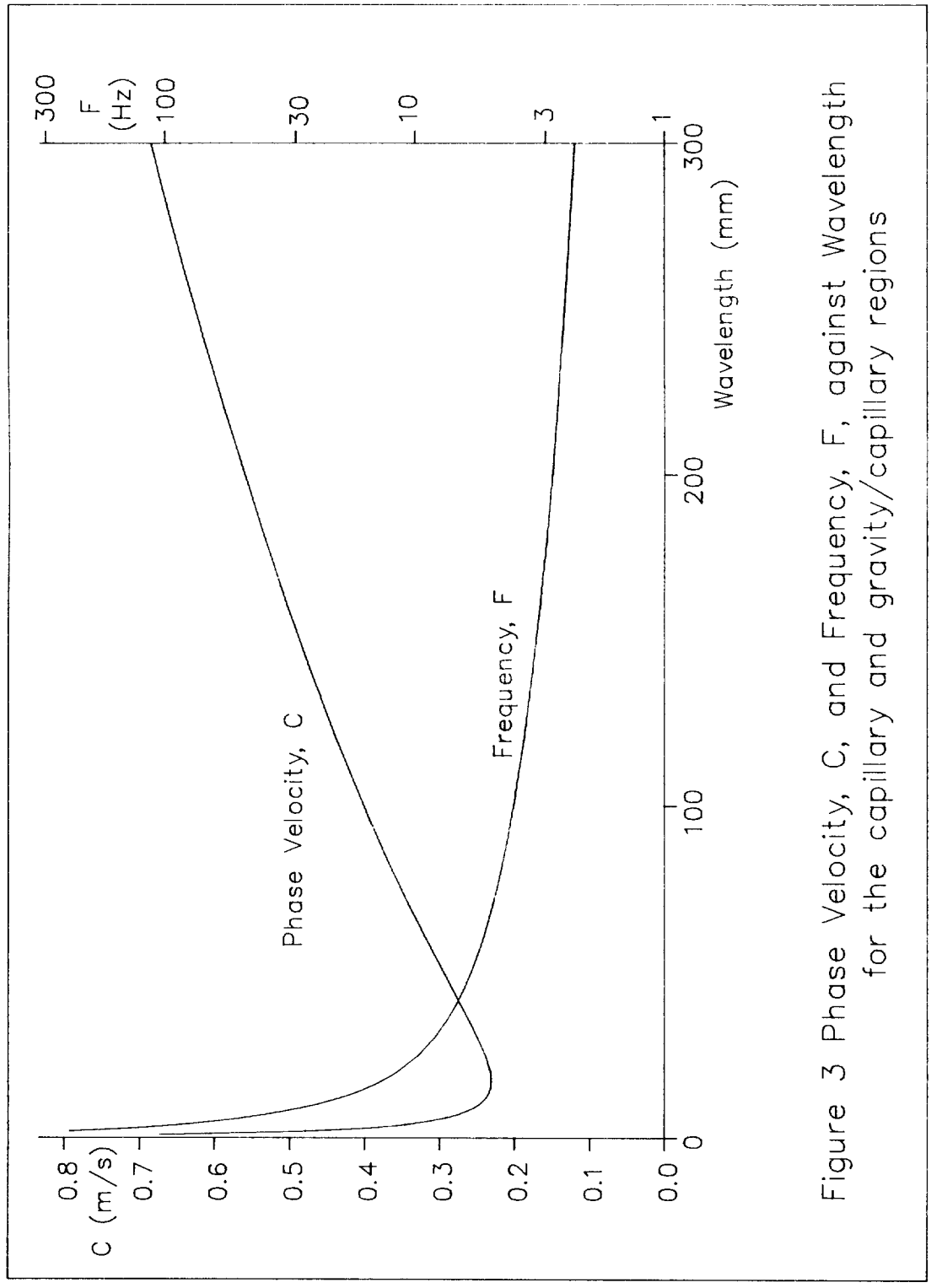

Figure 3 Phase Velocity, C, and Frequency, F, against Wavelength for the capillary and gravity/capillary regions

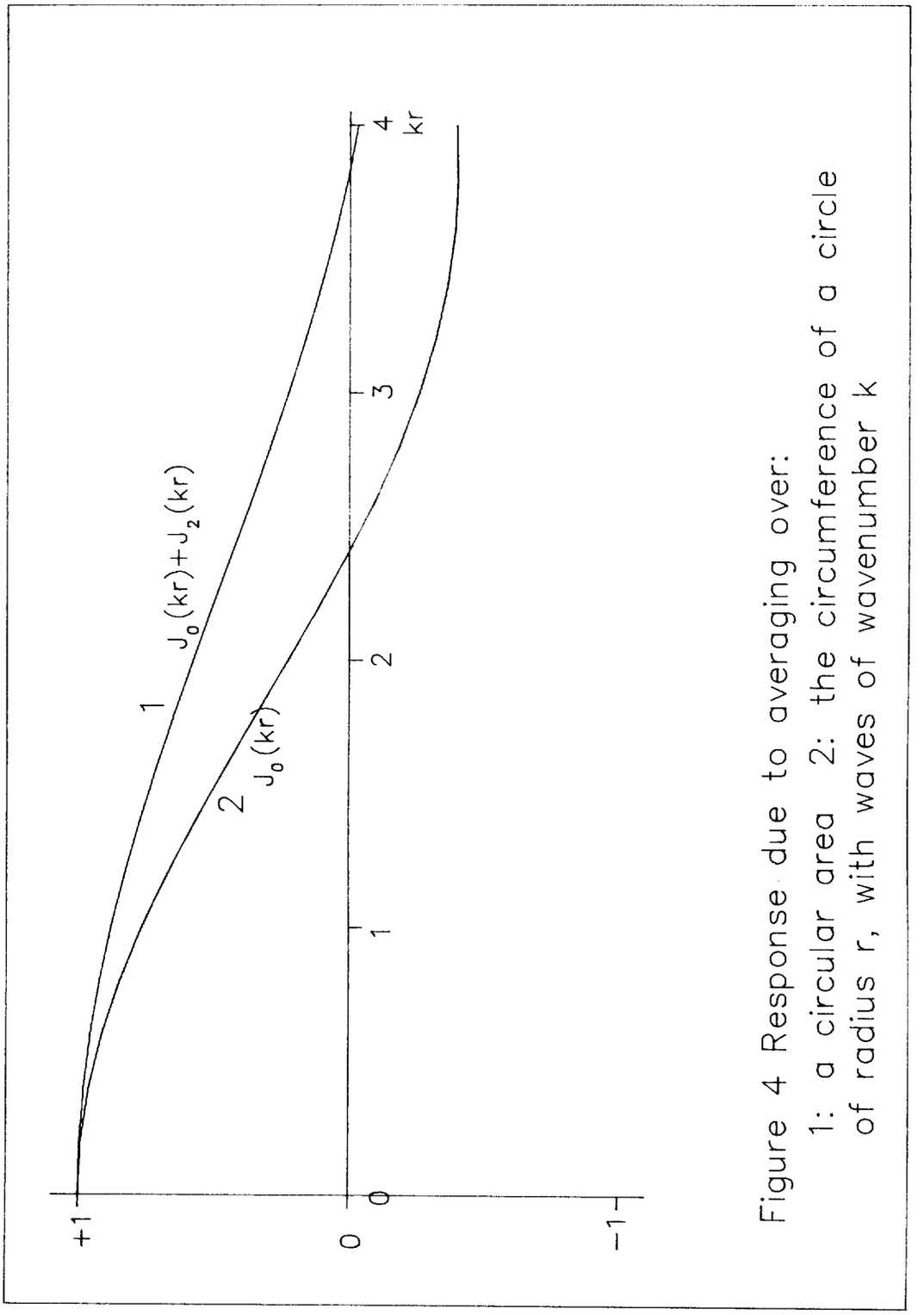

Figure 4 Response due to averaging over:
1: a circular area 2: the circumference of a circle
of radius r, with waves of wavenumber k

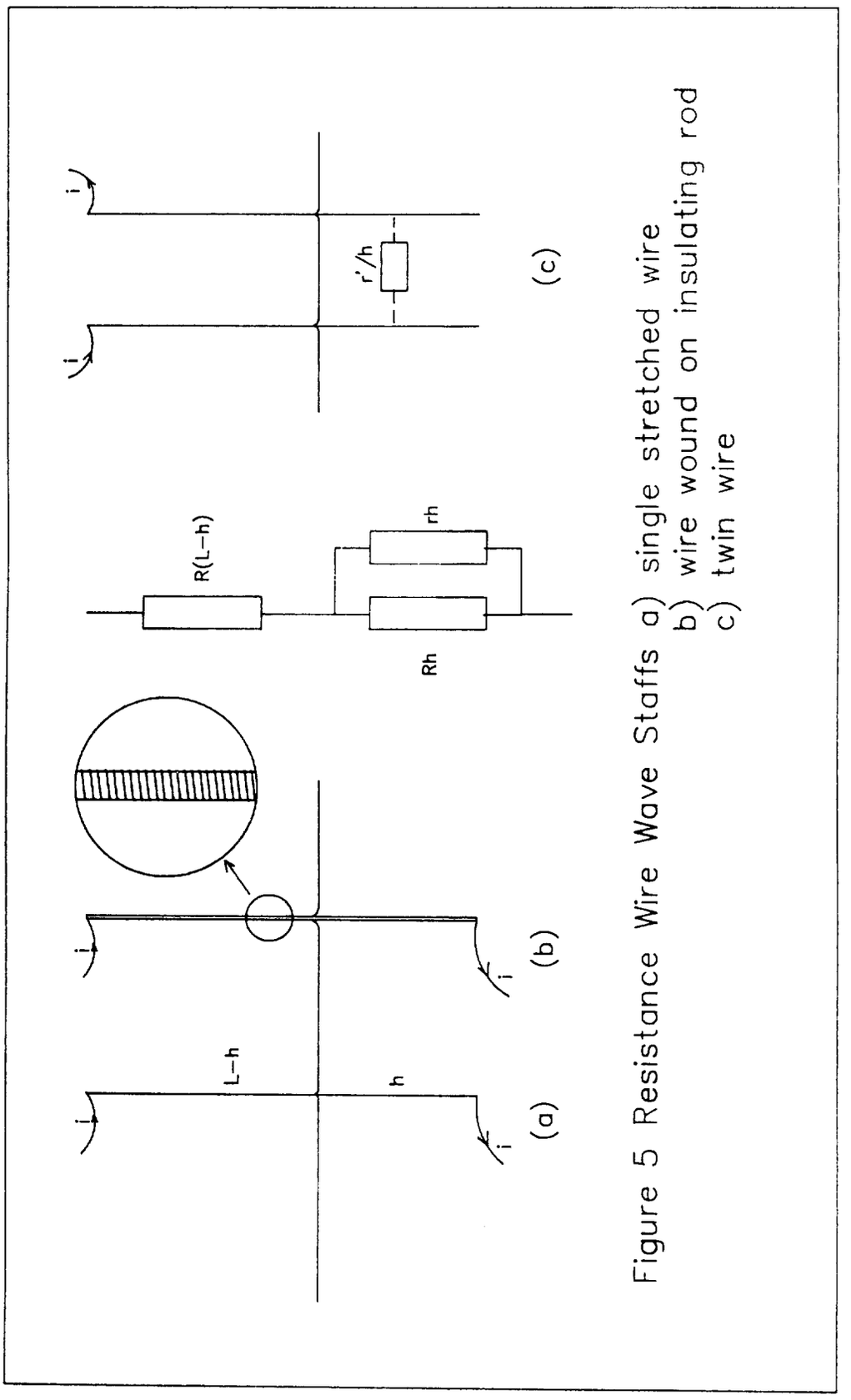

Figure 5 Resistance Wire Wave Staffs a) single stretched wire
b) wire wound on insulating rod
c) twin wire

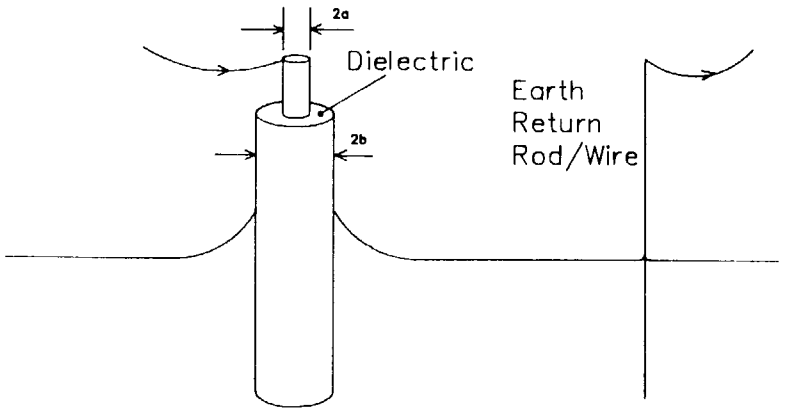

a) Capacitance Wire Wave Staff

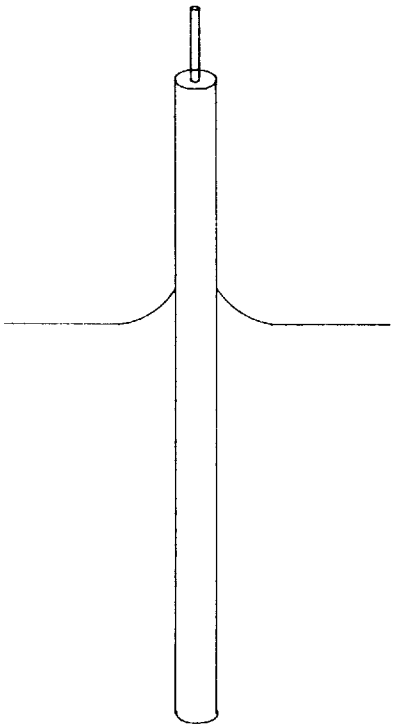

b) "GOUBAU" Line

Field Distribution

Figure 6 Capacitance Wire and Transmission Line Wave Staffs

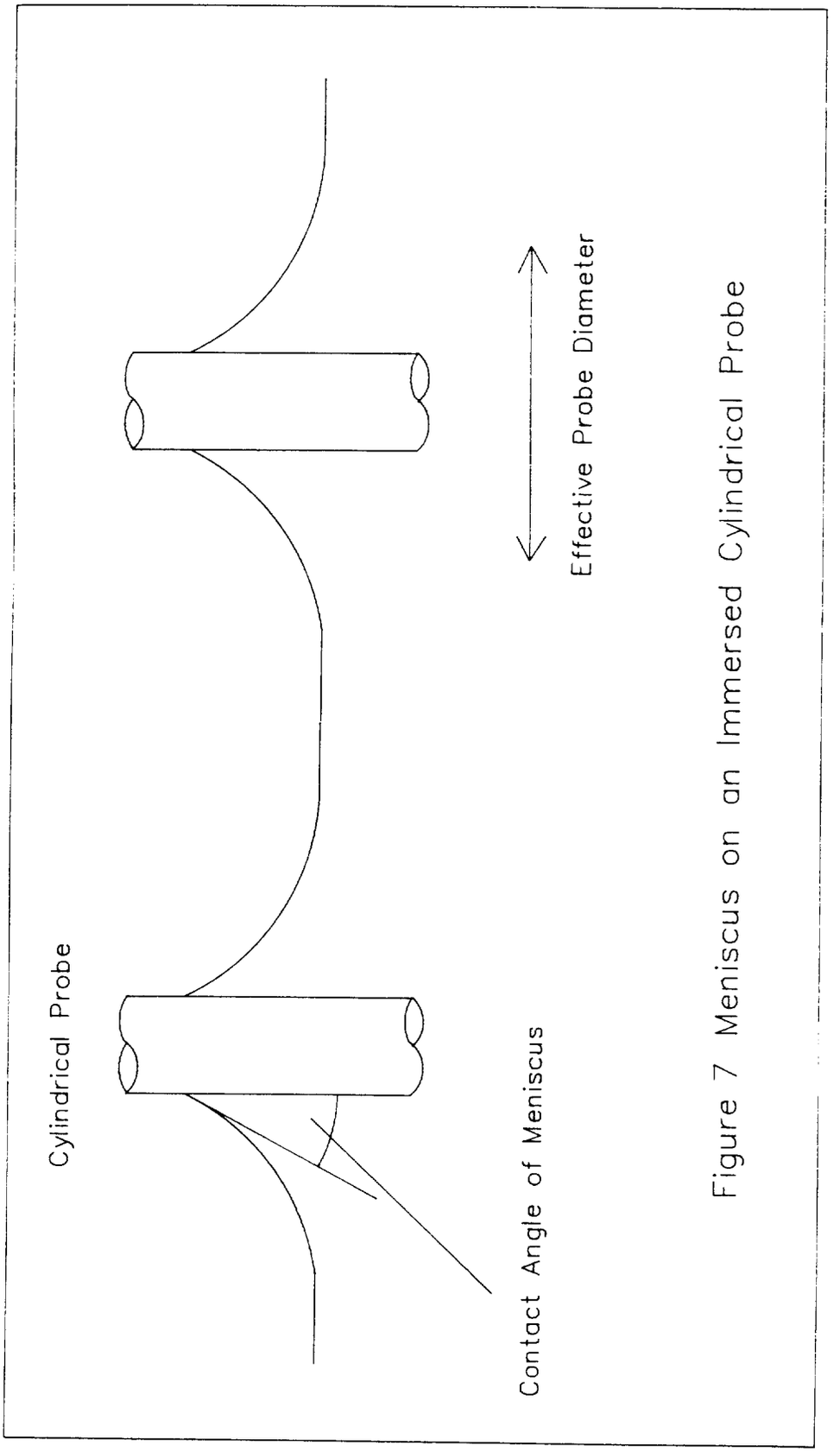

Figure 7 Meniscus on an Immersed Cylindrical Probe

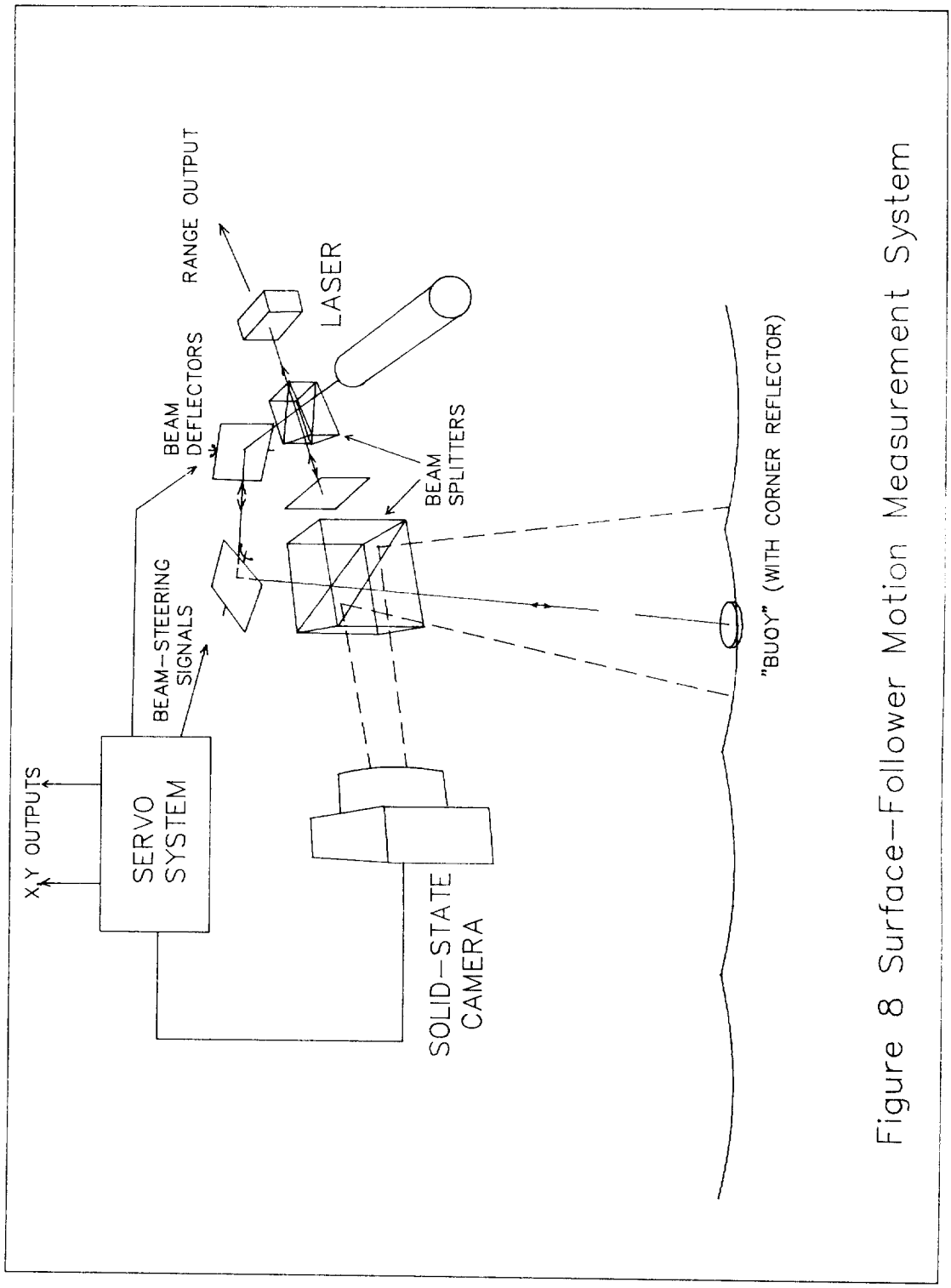

Figure 8 Surface-Follower Motion Measurement System

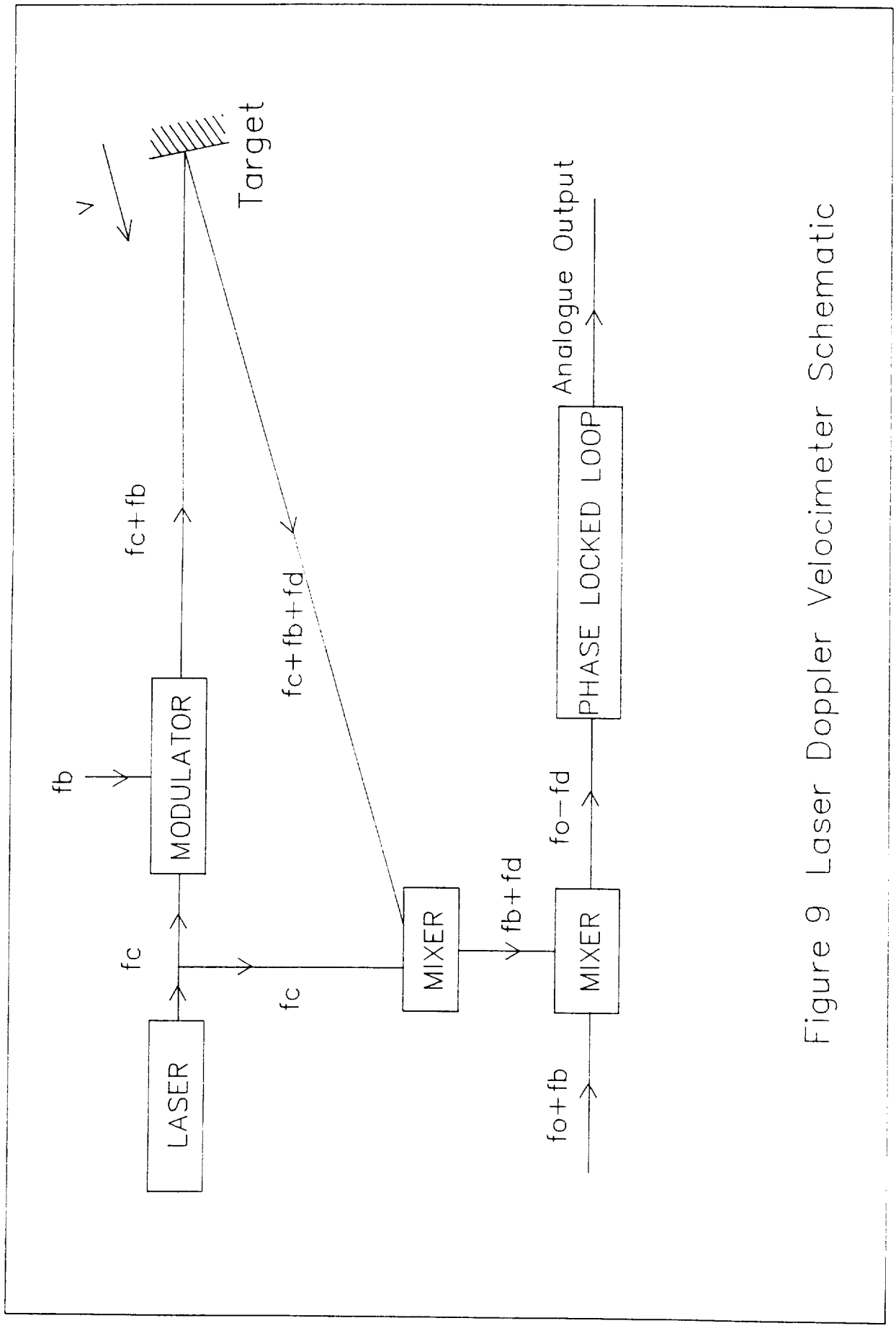

Figure 9 Laser Doppler Velocimeter Schematic

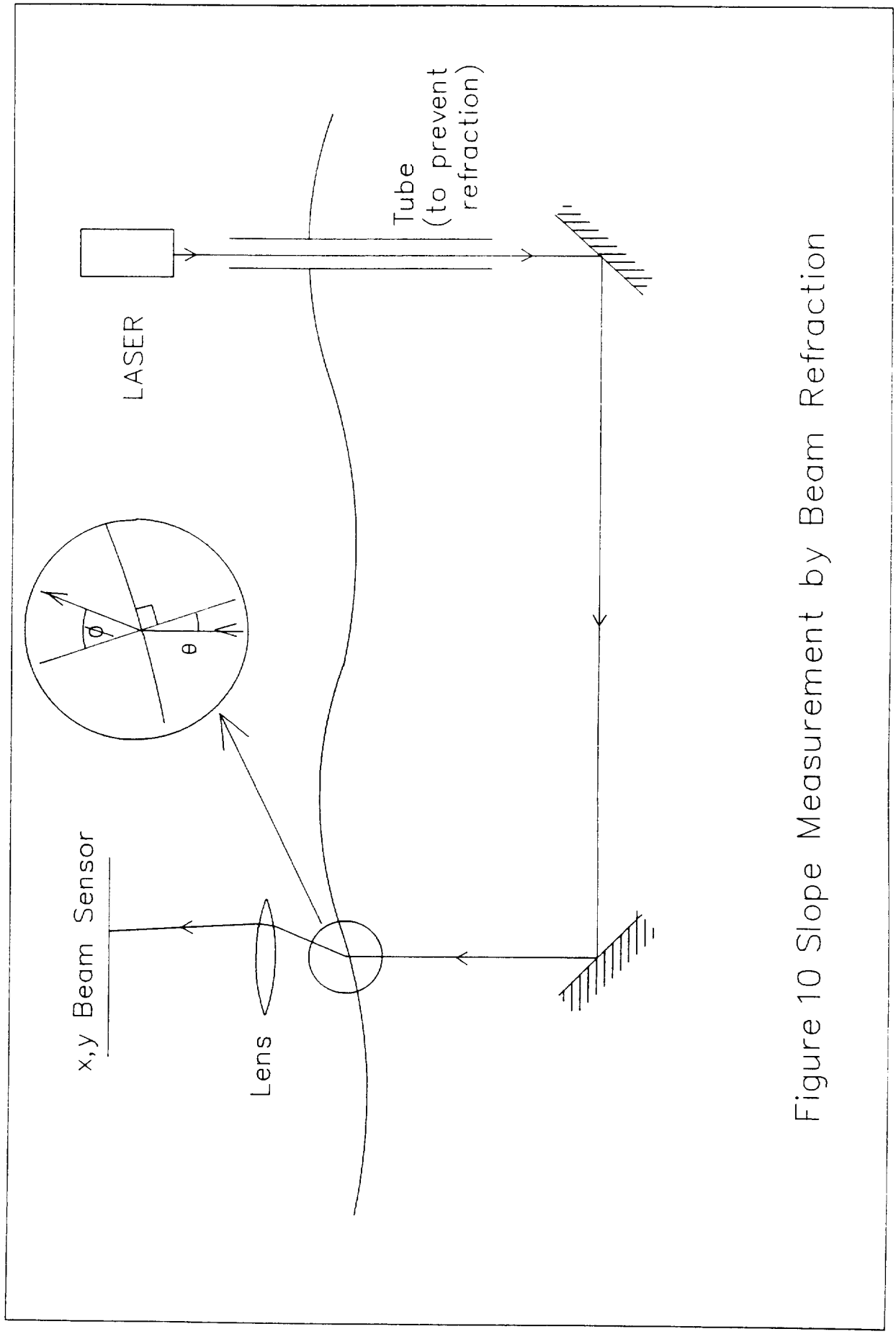

Figure 10 Slope Measurement by Beam Refraction

REFERENCES

ALTMANN, H. 1980 A water-wave height probe with calibration stabilised for changes in water conductivity.
Journal of Physics E : Scientific Instruments, 13, 390-392.

ALPERS, W. & HASSELMANN, K. 1978 The two-frequency microwave technique for measuring ocean wave spectra from an airplane or satellite.
Boundary-Layer Meteorology, 13, 215-230.

ALPERS, W. & JONES, W.L. 1978 The modulation of the radar backscattering cross section by long ocean waves.
pp.1597-1607 in, Proceedings of 12th International Symposium on Remote Sensing of Environment, Manila.

ALPERS, W.R., ROSS, D.B. & RUFENACH, C.L. 1981 On the detectability of ocean surface waves by real and synthetic aperture radar.
Journal of Geophysical Research, 86, 6481-6498.

ATAKTURK, S.S. & KATSAROS, K.B. 1987 Intrinsic frequency spectra of short gravity-capillary waves obtained from temporal measurements of wave height on a lake.
Journal of Geophysical Research, 92, 5131-5141.

ATANASSOV, V., ROSENTHAL, W. & ZIEMER, F. 1984 Removal of ambiguity oftwo-dimensional grey level variance spectra obtained by processing ship radar images of ocean waves.
In, Proceedings of IGARSS'84 Symposium, Strasbourg.
European Space Agency Special Publication 215, 333-336.

BAKER, W.F. 1970 A directional wave buoy for obtaining sea surface statistics up to 15 Hz.
Admiralty Underwater Weapons Establishment Technical Note 356/69 (unclassified), 16pp. + figures.

BANNER, M.L., JONES, I.S.F. & TRINDER, J.C. 1989 Wavenumber spectra of short gravity waves
Journal of Fluid Mechanics, 198, 321-344.

BARSTOW, S.F., KROGSTAD, H.E., TORSETHAUGEN, K. & AUDUNSON, T. 1985 Procedures and problems associated with the calibration of wave sensors.
pp.55-82 in, Advances in Underwater Technology and Offshore Engineering, Volume 4.
London: Graham & Trotman, 267pp.

BARNETT, T.P. & WILKERSON, J.C. 1967 On the generation of wind waves as inferred from airborne measurements of fetch-limited spectra.
Journal of Marine Research, 25, 292-328.

CHANG, P.C., GOROVE, A., ATCHLEY, R.L. & PLATE, E.J. 1970 A self-adjusting probe positioner for measuring flow fields in the vicinity of wind-generated water surface waves.
Review of Scientific Instruments, 41, 1544-1549.

CHANG, J.H., WAGNER, R.N. & YUEN, H.C. 1978 Measurement of high frequency capillary waves on steep gravity waves.
Journal of Fluid Mechanics, 86, 401-413.

COTE, L.J. *et al.* 1960 The directional spectrum of a wind generated sea as determined from data obtained by the Stereo Wave Observations Project.
Meteorological Papers, New York University, 2(6), 88pp.

COOKE, M.P. & DESA,A. 1982 A new method of non-contact measurement of linear displacement.
Journal of Physics E : Scientific Instruments, 15, 843-847.

COX, C.S. 1958 Measurements of slopes of high frequency wind-waves.
Journal of Marine Research, 16, 199-225.

COX, C.S. & MUNK, W.H. 1954 Measurements of the roughness of the sea surface from photographs of the sun's glitter.
Journal of the Optical Society of America, 44, 838-850.

CRABB, J.A., DRIVER, J.S. & HAINE, R.A. 1983 An intercomparison between six wave recorders at NMI Tower, Christchurch Bay.
Institute of Oceanographic Sciences Report No.154, 74pp.

CRAPPER, G.D. 1970 Non-linear capillary waves generated by steep gravity waves.
Journal of Fluid Mechanics, 40, 149-159.

DOBSON, E.B. 1970 Measurement of the fine-scale structure of the sea.
Journal of Geophysical Research, 75, 2853-2856.

DORMAN, C.E. & MOLLO-CHRISTENSEN, E. 1973 Observation of the structure of moving gust patterns over a water surface (cat's paws).
Journal of Physical Oceanography, 3, 120-132.

DURDEN, S.L. & VESECKY, J.F. 1985 A physical radar cross-section model for a wind-driven sea with swell.
IEEE Journal of Oceanic Engineering, OE-10, 445-451.

EVANS, D.D. & SHEMDIN, O.H. 1980 An investigation of the modulations of capillary and short gravity waves in the open ocean.
Journal of Geophysical Research, 85, 5019-5024.

EWING, J.A., CLAYSON, C.H., BIRCH, K.G. & PASCAL, R.W. 1984 Report on the measurement of high frequency waves.
Institute of Oceanographic Sciences Internal Document No. 212, 10pp. (unpublished manuscript).

FISCELLA, B., LOMBARDINI, P.P. & PAVESE, P. 1982 Interferential microwave probe for measuring sea ripples.
Il Nuovo Cimento, 5C, 247-255.

FISCELLA, B., LOMBARDINI, P.P., TRIVERO, P. & CAPPA, C. 1985 Sea return at C and Ku bands.
Il Nuovo Cimento, 10C, 381-385.

FRASER, D.C. 1966 Experiments to measure the magnetic fields of ocean waves in shallow water.
pp.15/1-15/5 in, Proceedings of I.E.R.E. Conference on Electronic Engineering in Oceanography, Southampton, 1966.
London: Institution of Electronic and Radio Engineers (IERE Conference Proceedings 8).

FRYER, D.D. & THOMAS, M.W.S. 1975 A linear twin wire probe for measuring water waves.
Journal of Physics E : Scientific Instruments, 8, 405-408.

GOTWOLS, B.L. & IRANI, G.B. 1980 Optical determination of the phase velocity of short gravity waves.
Journal of Geophysical Research, 85, 3964-3970.

GOTWOLS, B.L. & IRANI, G.B. 1982 Charge-coupled device camera system for remotely measuring the dynamics of ocean waves.
Applied Optics, 21, 851-860.

HAIMBACH, S.P. & WU, J. 1983 Simultaneous two-dimensional measurements of sea-surface slopes.
pp.9.1-9.5, in Proceedings of IGARSS'83 Symposium, San Francisco, Volume 1.
New York: IEEE.

HASSELMANN, K. *et al.* 1973 Measurements of wind wave growth during the Joint North Sea Wave Project (JONSWAP).
Erganzungschaft zur Deutschen Hydrographischen Zeitschrift, A, No. 12, 95pp.

HENDERSON, D.M. & HAMMACK, J.L. 1987 Experiments on ripple instabilities. Part 1. Resonant triads.
Journal of Fluid Mechanics, 184, 15-41.

HOGE, F.E. & SWIFT, R.N. 1980 Airborne oceanographic lidar (AOL) data acquisition modes and recent results.
NOAA Technical Memorandum ERL PMEL-18, 75-96.

HOGE, F.E. & SWIFT, R.N. 1980 Water depth measurement using an airborne pulsed neon laser system.
Applied Optics, 19, 871-887.

HOGE, F.E., KRABILL, W.B. & SWIFT, R.N. 1984 The reflection of airborne UV laser pulses from the ocean.
Marine Geodesy, 8, 313-344.

HUGHES, B.A., GRANT, H.L. & CHAPPEL, R.W. 1977 A fast response surface wave slope meter and measured wind-wave moments.
Deep Sea Research, 24, 1211-1223.

JONES, W.L., GRANTHAM, W.L., SCHROEDER, L.C., JOHNSON, J.W., SWIFT, C.T. & MITCHELL,J.L. 1975 Microwave scattering from the sea surface.
IEEE Transactions on Microwave Theory and Techniques, December 1975, 1053-1058.

JONES, W.L. & SCHROEDER, L.C. 1978 Radar backscatter from the ocean: dependence on surface friction velocity.
Boundary-Layer Meteorology, 13, 133-149.

KAHMA, K.K. & DONELAN, M.A. 1988 A laboratory study of the minimum wind speed for wind wave generation.
Journal of Fluid Mechanics, 192, 339-364.

KAYE, G.W.C. & LABY, T.H. 1966 Tables of physical and chemical constants, 13th ed.
London: Longmans, Green and Company.

KELLER, J.B. 1962 Geometrical theory of diffraction
Journal of the Optical Society of America, 52, 116-130.

KELLER, W.C., PLANT, W.J. & VALENZUELA, G.R. 1986 Observation of breaking waves with coherent microwave radar.
pp.285-293 in Wave Dynamics and Radio Probing of the Ocean Surface (ed. O.M. Phillips & K. Hasselmann).
New York: Plenum Press.

KINSMAN, B. 1965 Wind waves: their generation and propagation on the ocean surface.
Englewood Cliffs, NJ: Prentice Hall, 676pp.

KITAIGORODSKII, S.A. 1961 Applications of the theory of similarity to the analysis of wind generated wave motions as a stochastic process.
Bulletin of the Academy of Sciences USSR, Geophysics Series, No. 1, 73-80.

KITAIGORODSKII, S.A. 1973 The physics of air-sea interaction.
Jerusalem: Israel Program for Scientific Translation, 237pp.

KITAIGORODSKII, S.A. 1986 The equilibrium ranges in wind-wave spectra.
pp.9-40 in, Wave Dynamics and Radio Probing of the Ocean Surface (ed. O.M. Phillips & K. Hasselmann).
New York: Plenum Press.

KONDO, J., FUJINAWA, Y. & NAITO, G. 1973 High frequency components of ocean waves and their relation to the aerodynamic roughness.
Journal of Physical Oceanography, 3, 197-202.

KONYAYEV, K.V. & NAZAROV, A.A. 1970 The measurement of the space-time structure of the high frequency components of wind-driven swell.
Izvestiya Atmospheric and Oceanic Physics, 6, 58-61.

KRISHNAN, K.S. & PEPPERS, N.A. 1975 Remote optical methods to sense the ocean surface. pp.113-135 in, Proceedings of the International Symposium on Ocean Wave Measurement and Analysis,New Orleans, Vol. 2.
New York: American Society of Civil Engineers.

KRONENGOLD, M. LOWENSTEIN, J.M. & BERMAN, G.A. 1965 Sensors for theobservation of wave height and wind direction.
Marine Science Instrumentation, 13, 273-288.

KUO, E.Y.T. & GROSCH, C. 1972 Survey and comments on methods for measuring the spectra of ocean surface short wavelength gravity-capillary waves.
Ocean and Atmospheric Science Inc., Technical Report 72-084, 35pp.

KWOH, D.S.W. & LAKE, B.M. 1984 A deterministic, coherent, and dual-polarized laboratory study of microwave backscattering from water waves, Part I: short gravity waves without wind.
IEEE Journal of Oceanic Engineering, OE-9, 291-308.

KWOH, D.S.W. & LAKE, B.M. 1986 Microwave scattering from short gravity waves.
pp.443-447 in, Wave Dynamics and Radar Probing of the Ocean Surface (ed. O.M. Phillips & K. Hasselmann).
New York: Plenum Press.

LARSON, T.R. & WRIGHT, J.W. 1975 Wind-generated gravity-capillary waves: laboratory measurements of temporal growth rates using microwave backscatter.
Journal of Fluid Mechanics, 70, 417-436.

LAWNER, R.T. & MOORE, R.K. 1984 Short gravity and capillary wave spectra from tower-based radar.
IEEE Journal of Oceanic Engineering , OE-9, 317-324.

LEYKIN, I.A. & ROZENBERG, A.D. 1970 Study of the high-frequency part of the spetrum of an agitated sea.
Izvestiya Atmospheric and Oceanic Physics, 6, 1328-1332.

LEYKIN, I.A. & ROZENBERG, A.D. 1971 Measurement of the angular spectra of the high-frequency portion of swell.
Izvestiya Atmospheric and Oceanic Physics, 7, 102-106.

LIU, H-T. & LIN, J.-T. 1979 Effect of an oil slick on wind waves.
pp.665-674 in, Proceedings of 1979 Oil Spill Conference, Los Angeles.
Washington DC: American Petroleum Institute.

LIU, H-T. & LIN, J.-T. 1982 On the spectra of high frequency wind waves.
Journal of Fluid Mechanics, 123, 165-185.

LIU, P.C. & ROSS, D.B. 1980 Airborne measurements of wave growth for stable and unstable atmospheres in Lake Michigan.
Journal of Physical Oceanography, 10, 1842-1853.

LLEONART, G.T. & BLACKMAN, D.R. 1980 The spectral characteristics of wind-generated capillary waves.
Journal of Fluid Mechanics, 97, 455-479.

LOBEMEIER, P. 1981 A wire probe for measuring high frequency sea waves.
Journal of Physics E : Scientific Instruments, 14, 1407-1410.

LONG, S.R. & HUANG, N.E. 1976 On the variation and growth of wave-slope spectra in the capillary-gravity range with increasing wind.
Journal of Fluid Mechanics, 77, 209-228.

LONGUET-HIGGINS, M.S. 1963 The generation of capillary waves by steep gravity waves.
Journal of Fluid Mechanics, 16, 138-159.

LONGUET-HIGGINS, M.S. 1986 Eulerian and Lagrangian aspects of surface waves.
Journal of Fluid Mechanics, 173, 683-707.

LUBARD, S.C., KRIMMEL, J.E., THEBAUD, L.R., EVANS, D.D. & SHEMDIN, O.H. 1980 Optical image and laser slope meter intercomparisons of high frequency waves.
Journal of Geophysical Research, 85, 4996-5002.

McILWRAITH,.C.G. & HAYS, S.D. 1963 Ocean wave measurement by sonar.
Journal of Marine Research, 21, 94-101.

McCLAIN, C.R., HUANG, N.E. & LAVIOLETTE, P.E. 1982 Measurements of the sea state variation across oceanic fronts using laser profilometry.
Journal of Physical Oceanography, 12, 1228-1244.

MASUKO, H., OKAMOTO, K., YOSHIKADO, S. & TAKASUGI, T. 1984 Measurements of microwave back-scattering signatures of the ocean surface using X-band and Ka-band airborne scatterometer/radiometer system.
In, Proceedings of IGARSS'84 Symposium, Strasbourg.
European Space Agency Special Publication 215.

MELVILLE, W.K. & RAPP, R.J. 1988 The surface velocity field in steep and breaking waves.
Journal of Fluid Mechanics, 189, 1-22.

MILLER, L.S. & PARSONS, C.L. 1985 The effect of microwave backscatter uncertainty on satellite radar altimeter accuracy.
IEEE Journal of Oceanic Engineering, OE-10, 438-442.

MITSUYASU, H. & HONDA, T. 1974 The high frequency spectrum of wind-generated waves.
Journal of Oceanographical Society of Japan, 30, 185-198.

MITSUYASU, H. & HONDA, T. 1975 The high frequency spectrum of wind generated waves.
Reports of Research Institute for Applied Mechanics, 71, 327-355.

MITSUYASU, H. 1977 Measurement of the high-frequency spectrum of ocean surface waves.
Journal of Physical Oceanography, 7, 882-891.

MONALDO, F.M. & KASEVCIH, R.S. 1981 Measurement of shoret wave modulation using fine series optical spectra.
Journal of Physical Oceanography, 11, 1034-1036.

MONALDO, F.M. & KASEVICH, R.S. 1982 Optical determination of short wave modulation by long waves.
IEEE Transactions on Geoscience and Remote Sensing, GE-20, 254-258.

OLSEN, W.S. & ADAMS, R.M. 1970 A laser profilometer.
Journal of Geophysical Research, 75, 2185-2187.

PALM, C.S., ANDERSON, R.C. & REECE, A.M. 1977 Laser probe for measuring 2-D wave slope spectra of ocean capillary waves.
Applied Optics, 16, 1074-1081.

PHILLIPS, O.M. 1958 The equilibrium range in the spectrum ofwind-generated ocean waves.
Journal of Fluid Mechanics, 4, 426-434.

PHILLIPS, O.M. 1977 The dynamics of the upper ocean.
Cambridge: Cambridge University Press, 336pp.

PHILLIPS, O.M. 1985 Spectral and statistical properties of the equilibrium range in wind-generated gravity waves.
Journal of Fluid Mechanics, 156, 505-531.

PIERSON, W.J. & STACY, R.A. 1973 The elevation, slope and curvature spectra of wind roughened sea surface.
NASA Contractor Report CR-2247, 388pp.

PIERSON, W.J. 1976 The theory and applications of ocean wave measuring systems at and below the sea surface, on the land, from aircraft, and from spacecraft.
NASA Contractor Report CR-2646, 400pp.

PITT, E.G., DRIVER, J.S. & EWING, J.A. 1978 Some intercomparisons between wave recorders.
Institute of Oceanographic Sciences Report No. 43, 63pp.

PODNEY, W. 1975 Electromagnetic fields generated by ocean waves.
Journal of Geophysical Research, 80, 2977-2990.

PRETTYMAN, C.E. & CERMAK, M.D. 1969 Time variation of the rough ocean surface and its effect on an incident laser beam.
IEEE Transactions on Geoscience GE-7, 235-243.

REECE, A.M. & SHEMDIN, O.H. 1974 Modulation of capillary waves by long waves.
pp.82-92 in, Proceedings of the International Symposium on Ocean Wave Measurement and Analysis, New Orleans, No. 2.
New York: American Society of Civil Engineers.

REECE, A.M. 1978 Modulation of short waves by long waves.
Boundary-Layer Meteorology, 13, 203-214.

RICHTER, K. & ROSENTHAL, W. 1986 Energy distribution of waves above 1 Hz on long wind waves.
pp.75-93 in, Wave Dynamics and Radar Probing of the Ocean Surface (ed. O.M. Phillips & K Hasselmann).
New York: Plenum Press.

ROSS, D.B., CARDONE, V.J. & CONWAY, J.W.Jr. 1970 Laser and microwave observations of sea surface conditions for fetch-limited 17 to 25 m/s winds.
IEEE Transations on Geoscience Instrumentation, GE-8, 326-336.

SANCHOLUZ,A.G. 1978 A precise instrument for measuring water waves.
IEEE Transactions on Instrumentation and Measurement, IM-27, 281-284.

SCHOOLEY, A.H. 1962 Upwind-downwind ratio of radar returns calculated from facet size statistics of a wind-disturbed water surface.
Proceedings of the I.E.R.E., 50, 456-461.

SCHROEDER, L.C., SCHAFFNER, P.R., MITCHELL, J.L. & JONES, W.L. 1985 AAFE RADSCAT 13.9-GHz Measurements and analysis: wind-speed signature of the ocean.
IEEE Journal of Oceanic Engineering, OE-10, 346-357.

SCHULE, J.J., SIMPSON, L.S. & DELEONIBUS, P.S. 1971 A study of fetch-limited wave spectra with an airborne laser.
Journal of Geophysical Research, 76, 4160-4171.

SHEMDIN, O.H. & HSU, E.Y. 1967 Direct measurement of aerodynamic pressure above a simple progressive gravity wave.
Journal of Fluid Mechanics, 30, 403-416.

SHEMDIN, O.H. & TOBER, G. 1980 Surface followers.
pp.627-644 in, Air-Sea Interaction: instruments and methods (ed. F. Dobson, L. Hasse & R. Davies.
New York: Plenum Press.

SHEMDIN, O.H., TRAN, H.M. & WU, S.C. 1988 Directional measurement of short ocean waves with stereophotography.
Journal of Geophysical Research, 93, 13891-13901

SHUTKO, A.M. 1985 The status of the passive microwave sensing of the waters- lakes, seas and oceans - under the variation of their state, temperature, and mineralisation (salinity): models, experiments, examples of application.
IEEE Journal of Oceanic Engineering, OE-10, 418-437.

SKOLNIK, M.I. 1970 Sea Echo.
pp.26.1-26.3 in, Radar Handbook (ed. M.I. Skolnik).
New York: McGraw-Hill.

SMITH, C.J. 1960 A Degree Physics, Part III. Optics.
London: Edward Arnold, 736pp.

SPINDEL, R.C. & SCHULTHEISS, P.M. 1971 Two-dimensional probability structure of wind-driven waves.
Journal of the Acoustical Society of America, 52, 1065-1068.

STACY, R.A. 1974 Spectral analyses of high frequency gravity waves generated by a hurricane.
New York University, School of Engineering and Science, Ph.D Thesis.

STILWELL, D. 1969 Directional energy spectra of the sea from photographs.
Journal of Geophysical Research, 74, 1974-1986.

STILWELL, D. & PILON, R.O. 1974 Directional spectra of surface waves from photographs.
Journal of Geophysical Research, 79, 1277-1284.

STURM, G.V. & SORRELL, F.Y. 1973 Optical measurement technique and experimental comparison with wave height probes.
Applied Optics, 12, 1928-1933.

TANG, S. & SHEMDIN, O.H. 1983 Measurement of high frequency waves using a wave follower
Journal of Geophysical Research, 88, 9832-9840.

TANG, S. & SHEMDIN, O.H. 1983 Measurement of high frequency waves using a wave follower.
Journal of Geophysical Research, 88, 9832-9840.

THOMAS, M.H.B. 1980 The physical basis of remote sensing measurements at sea.
AERE Harwell Report R9770, 34pp. + figures.

TOBA, Y. 1973 Local balance in the air-sea boundary processes. III. On the spectrum of wind waves.
Journal of the Oceanographical Society of Japan, 29, 209-220.

TOBER, G., ANDERSON, R.C. & SHEMDIN, O.H. 1973 Laser instrument for detecting water ripple slopes.
Applied Optics, 12, 788-794.

TRIVERO, P. & CAPPA, C. 1987 Sea wave spectra by electromagnetic techniques.
Il Nuovo Cimento, 10C, 409-418.

TRIZNA, D.B. 1985 A model for doppler peak spectral shift for low grazing angle sea scatter.
IEEE Journal of Oceanic Engineering, OE-10, 368-375.

VALENZUELA, G.R. 1968 Scattering of electromagnetic waves from a tilted slightly rough surface.
Radio Science, 3, 1057-1066.

VALENZUELA, G.R. 1978 Theories for the interaction of electromagnetic and ocean waves - a review.
Boundary-Layer Meteorology, 13, 61-85.

WALSH, E.J., HANCOCK, D.W., HINES, D.E., SWIFT, R.N. & SCOTT, J.F. 1985 Elimination of directional wave spectrum contamination from noise in elevation measurements.
IEEE Journal of Oceanic Engineering, OE-10, 376-381.

WEAVER,J.T. 1965 Magnetic variations associated with ocean waves and swell.
Journal of Geophysical Research, 70, 1921-1929.

WHITE, D.A. & TALLMADGE, J.A. 1965 Static menisci on the outside of cylinders.
Journal of Fluid Mechanics, 23, 325-336.

WRIGHT, J.W. 1966 Backscattering from capillary waves with application to sea clutter.
I.E.E.E. Transactions on Antennae and Propagation, 14, 749-754.

WRIGHT, J.W. 1978 Detection of ocean waves by microwave radar; the modulation of short gravity-capillary waves.
Boundary-Layer Meteorology, 13, 87-105.

WU, J. 1971 Slope and curvature distributions of wind-disturbed water surface.
Journal of the Optical Society of America, 61, 852-858.

WU, J. 1977 Directional slope and curvature distributions of wind waves.
Journal of Fluid Mechanics, 79, 463-480.

YOUNG, I.R., ROSENTHAL, W. & ZIEMER, F. 1984 A three-dimensional description of the sea surface by means of marine navigational radar.
In, Proceedings of IGARRS'84 Symposium, Strasbourg.
European Space Agency Special Publication 215, 315-319.

ZWARTS, C.M.G. 1975 A transmission line wave height and level transducer.
Quarterly Bulletin of the Division of Mechanical Engineering, National Research Council of Canada, No.1, 1-23.

APPENDIX A

Sensor Response due to Spatial Averaging

(a) Averaging over a circular area (Figure A.1)

Assume a unidirectional wave, such that the surface displacement, ζ, is given by

$$\zeta = 0.5H.\sin(kx-\psi)$$

where $\psi = \omega t + \phi$.

The sensor output will then be given by

$$o/p = \frac{1}{\pi r^2}\int_0^{\pi} 2r.\sin\theta.r.\sin\theta.d\theta.\zeta$$

$$= \frac{H}{2\pi}\int_{\pi}^{o} (\sin(kr.\cos\theta).\cos\psi+\cos(kr.\cos\theta).\sin\psi)(\cos2\theta-1).d\theta$$

$$= (J_o(kr)+J_2(kr)).0.5H\sin(-\psi)$$

$$= (J_o(kr) + J_2(kr)).\zeta(x = 0)$$

i.e. the sensor response is given by $(J_o(kr)+J_2(kr))$.

(b) Averaging over a circular circumference (Figure A.2)

The sensor output will be given by

$$o/p = \frac{1}{2\pi r}\int_0^{\pi} 2r.d\theta.\zeta$$

$$= \frac{H}{2\pi}\int_0^{\pi}(\sin(kr.\cos\theta).\cos\psi+\cos(kr.\cos\theta).\sin\psi).d\theta$$

$$= J_o(kr).\zeta(x = 0)$$

i.e. the sensor response will be given by $J_o(kr)$.

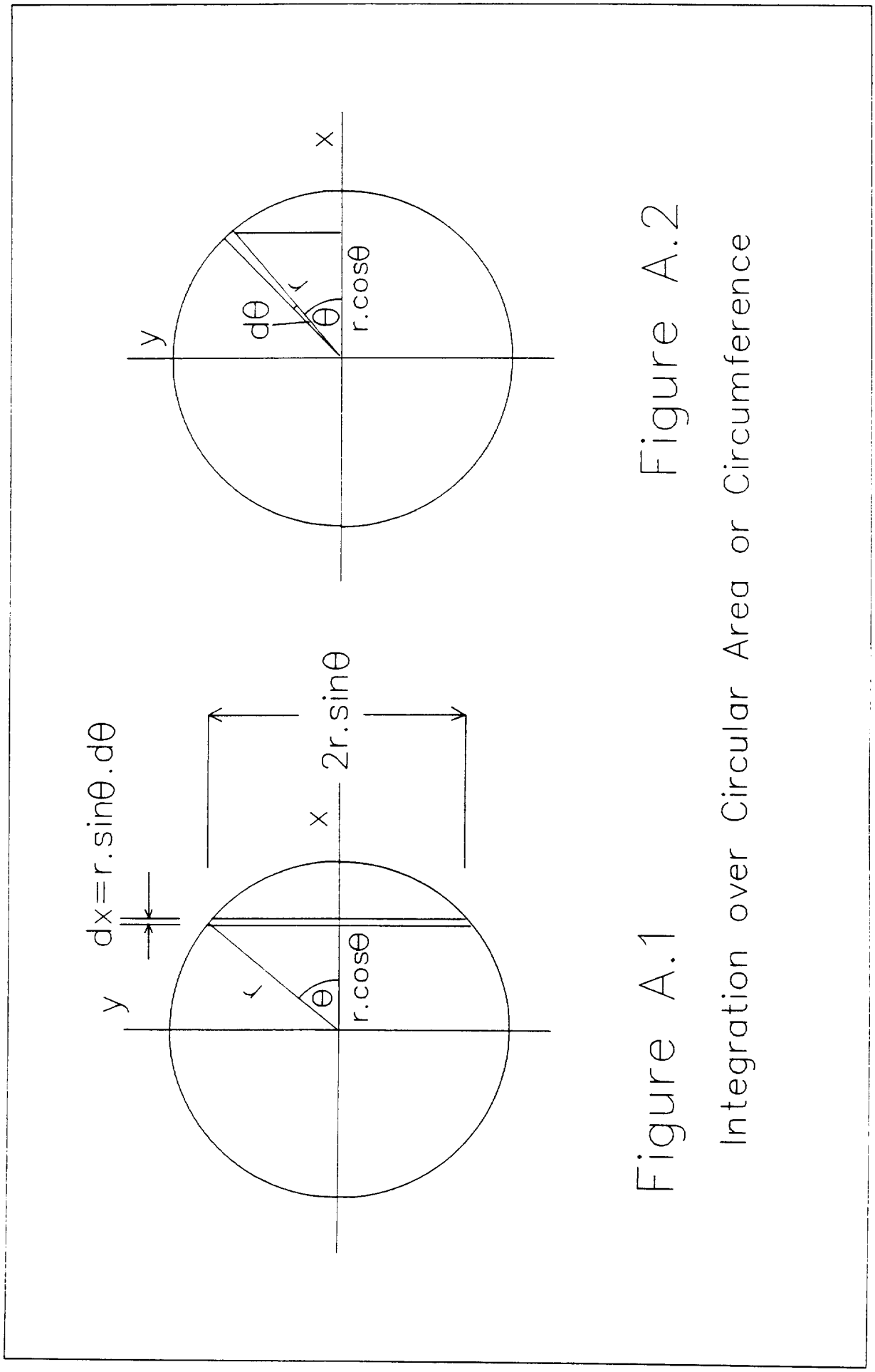

Figure A.1

Figure A.2

Integration over Circular Area or Circumference

APPENDIX B

Beamwidth-related Distortion in Radars/Inverted Echo Sounders

If we consider a unidirectional surface wave of elevation ζ, where

$$\zeta(x,y,t) = \frac{H}{2}.\ \sin(kx-\psi)$$

and $\psi = \omega t+\phi$

a radar or sonar with finite width beam, centred on the z-axis, will result in a distorted version of the vertical wave displacement $\zeta(t)$. For simplicity we assume that the water surface is a good isotropic scatterer at the radar/sonar wavelength and that the radiation pattern of the radar/sonar is uniform over a cone of half angle θ_b and zero outside this cone. Thus received signal threshold considerations are not relevant and one is only concerned with the shortest return path from the antenna/transducer to the water surface. In the case of a unidirectional water wave, this path will lie in a plane including the vertical and the direction of propagation of the wave (Figure B.1).

For a return path at angle θ, we have

$$\tan\theta = \frac{x}{D + \zeta(x,0,t)}$$

$$\text{i.e. } D + \frac{H}{2}.\ \sin(kx-\psi) = x.\cot\theta$$

The return path length, R, is then given by

$$R = 2x.\mathrm{cosec}\theta$$

The shortest return path length, $R_{min}(\psi)$, which gives the radar/sonar range, was calculated by successive approximation technique on a computer for various values of θ_b over a complete cycle of the water wave ($\psi = 0$ to 2π).

The distortion was then calculated by performing a Fourier analysis of $R_{min}(\psi)$ for the first three harmonics only. The result of this is shown in Figure B.2, where the amplitudes of the first three harmonics are plotted against the ratio of the width of the illuminated/insonified area to the water wavelength.

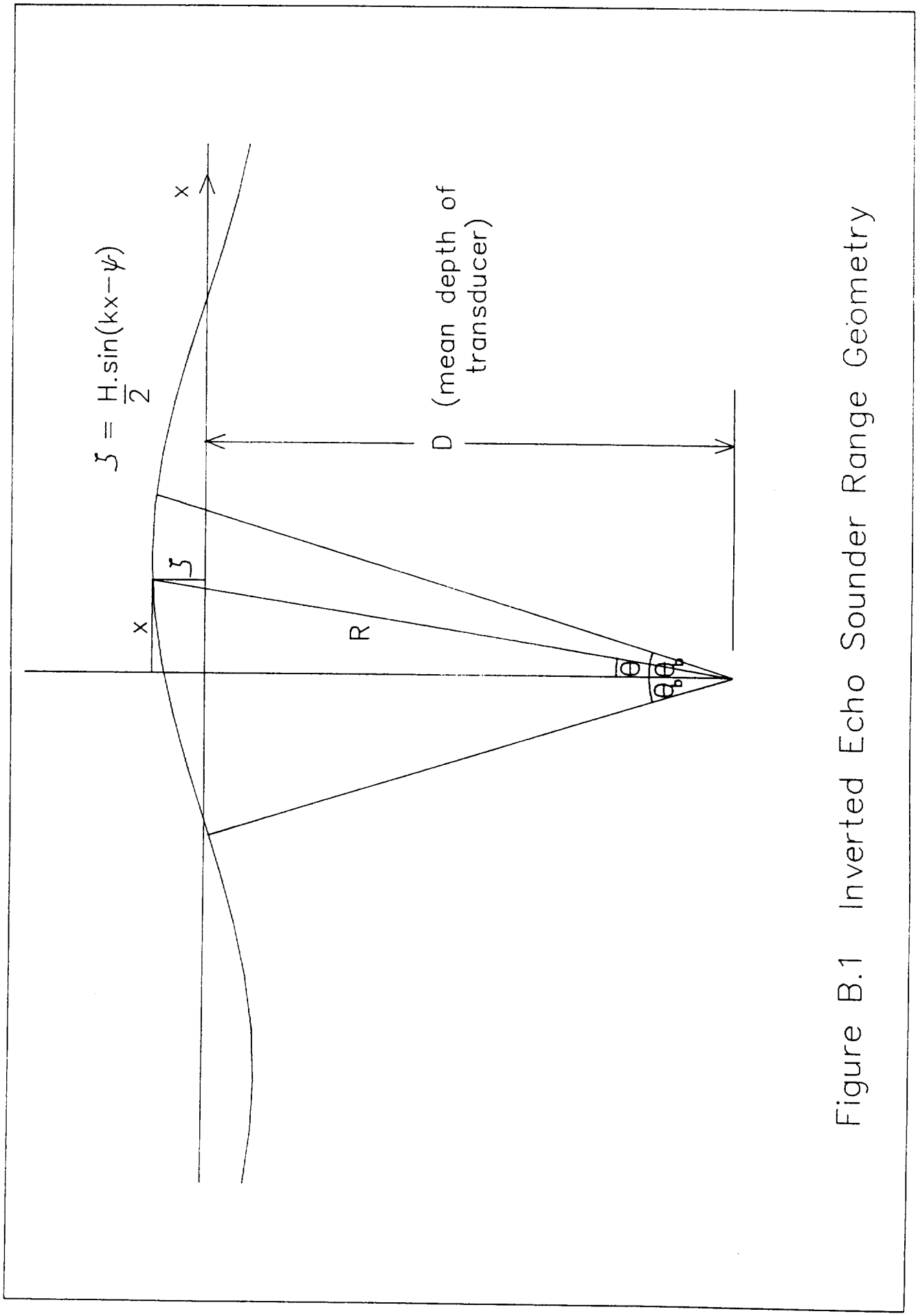

Figure B.1 Inverted Echo Sounder Range Geometry

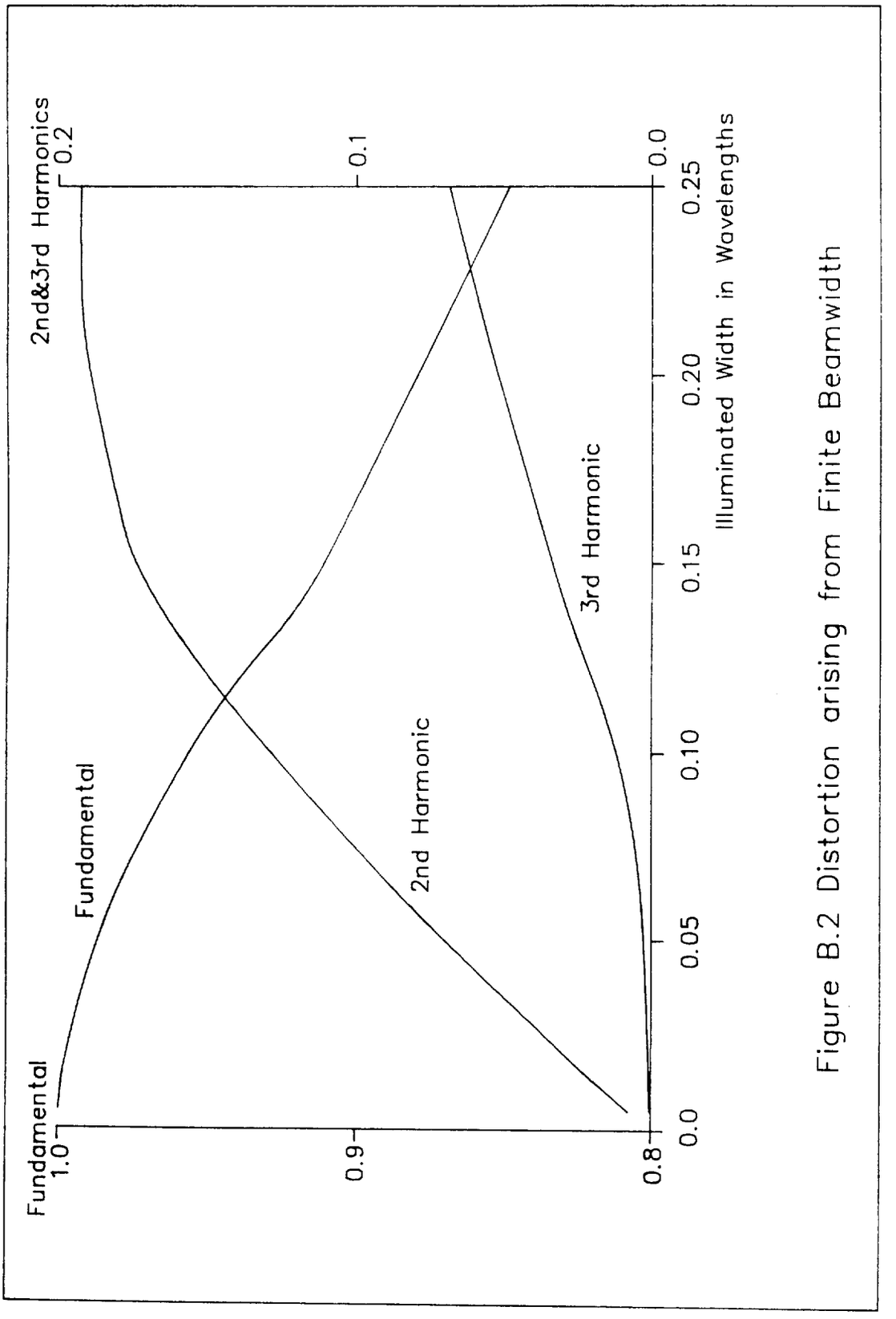

Figure B.2 Distortion arising from Finite Beamwidth